

Recent results of the study of ADS with 500 kg natural uranium target assembly QUINTA irradiated by deuterons with energies from 1 to 8 GeV at JINR NUCLOTRON

¹ W. Furman, J. Adam, A. Baldin, A. Berlev, N. Gundorin, Zh. Hushvaktov, M. Kadykov, Yu. Kopatch, E. Kostyukhov, Kudashkin, A. Makan'kin, I. Mar'in, A. Polansky, V. Pronskikh, A. Rogov, V. Schegolev, A. Solnyshkin, V. Tsupko-Sitnikov, S. Tyutyunnikov, A. Vishnevsky, N. Vladimirova, A. Wojciechowski, L. Zavorka

Joint institute for nuclear research,

Joliot Curie str.6, Dubna Moscow region, 141980 Russia

E-mail: furman@dubna.ru, iadam@jinr.ru, an.baldin@mail.ru, berlev@inr.ru, gundorin@nf.jinr.ru, khushvaktov@mail.ru, kadykov@jinr.ru, kopatch@nf.jinr.ru, kostyukhov@sunse.jinr.ru, kudashkin@sunse.jinr.ru, makankin@sunse.jinr.ru, mariin@sunse.jinr.ru, polanski@jinr.ru, soln@jinr.ru, vspron@fnal.gov, aurogov@nf.jinr.ru, vys@jinr.ru, vtsoupko@jinr.ru, tsi@sunse.jinr.ru, alex.vishnevskiy@mail.ru, nmvladi@mail.ru, andrzej@cyf.gov.pl, zavorka@jinr.ru

V. Chilap, A. Chinenov, B. Dubinkin, B. Fonarev, M. Galanin, V. Kolesnikov, S. Solodchenkova

Center Physical and Technical Projects "Atomenergomash",

Klara Cetkin str. 33, Moscow, 125130 Russia

E-mail: chilap@cftp-aem.ru, chinenov@cftp-aem.ru, boris.dubinkin@mail.ru, fonarev@atomem.ru, galanin@cftp-aem.ru, kolesnikov@atomem.ru, solod@cftp-aem.ru

M. Artyushenko, V. Sotnikov, V. Voronko

NSC Kharkov Institute of Physics and Technology,

Akademicheskaya str. 1, Kharkov, 61108 Ukraine

E-mail: art@kipt.kharkov.ua, sotnik@kipt.kharkov.ua, voronko@kipt.kharkov.ua

1

Speaker W. Furman

A. Khilmanovich, B. Martsynkevich

Stepanov Institute of Physics,

Nezavisimosti av. 68, Minsk, 220072 Belarus

E-mail: khilmanv@dragon.bas-net.by, martsyn48@gmail.com

S. Kislitsin, T. Kvochkina, S. Zhdanov

Institute of Nuclear Physics,

Ibragimova str. 1, 050032 Almaty, Kazakhstan

E-mail: skislitsin@inp.kz, kvochkina@inp.kz, sv.zhdanov@rambler.ru

K. Husak, S. Korneev, A. Potapenko, A. Safronova, I. Zhuk

Joint Institute for Power and Nuclear Research- Sosny near Minsk,

Academician Krasin str. 99, Minsk, 220109 Belarus

*E-mail: stikrina@mail.ru, s.korneyev@sosny.bas-net.by,
a.potapenko@tut.by, nastia84@mail.ru, zhuk@sosny.bas-net.by*

M. Suchopar, O. Svoboda, J. Vrzalova, V. Wagner

Nuclear Physics Institute, Rez near Prague,

25068 Řež, Czech Republic

*E-mail: suchopar@ujf.cas.cz, svoboda@ujf.cas.cz, vrzalova@ujf.cas.cz,
wagner@ujf.cas.cz*

L. Kostov, Ch. Stoyanov, P. Zhivkov

Institute of Nuclear Research and Nuclear Energy of Bulgarian Academy of Sciences,

Tzarigradsko chaussee, 72, Sofia, 1784 Bulgaria

*E-mail: lkostov@inrne.bas.bg, stoyanov@inrne.bas.bg,
petar.zhivkov@gmail.com*

M. Bielewicz, S. Kilim, E. Strugalska-Gola, M. Szuta

National Centre for Nuclear Research,

Pracownia Fizyki Jadrowej Stosowanej B3/3S, 04-500 Otwock-Swierk, Poland

*E-mail: m.bielewicz@cyf.gov.pl, s.kilim@cyf.gov.pl, elasg@cyf.gov.pl,
mszuta@cyf.gov.pl*

W. Westmeier

Gesellschaft für Kernspektrometrie,

Ebsdorfergrund-Mölln, Germany

E-mail: westmeier@t-online.de

M. Manolopoulou

*Aristotle Uni-Thessaloniki,
Thessaloniki, 54124 Greece
E-mail: metaxia@auth.gr*

S.R. Hashemi-Nezhad

*School of Physics, University of Sydney,
NSW 2006 | Australia
E-mail: reza@physics.usyd.edu.au*

The study of basic properties of the ADS presented in the previous Baldin seminar [1] was continued during the 2011-2012. For these experiments, uranium target assembly has been upgraded: the entrance window was created to reduce the albedo of the incident beam and a section was added to keep the effective mass of uranium to the beam axis. The new target assembly with a mass of 500 kg of natural uranium metal (diameter ~30cm and length 65cm) was named QUINTA. During the three runs of JINR NUCLOTRON the target assembly (TA) QUINTA was irradiated by deuterons with energies from 1 to 8 GeV and the total number of deuterons on the target of $(3-5) 10^{13}$ for each energy.

The the energy spectra of prompt neutrons inside and outside the target assembly and the time spectra of delayed neutrons (DN) between accelerator bursts were measured. Beside that the spatial distributions of fission rates inside TA have been measured with aid of solid state track detectors and independently by activation method. The last method was used for measurements of ^{239}Pu nuclei production. All these measurements were made with the original TA QUINTA as well as with TA surrounded by a 10 cm thick lead blanket.

Total numbers of fissions and produced ^{239}Pu nuclei were obtained by integration over QUINTA volume and normalized to one incident deuteron and one GeV. Both these numbers were constant within experimental errors of about 15 % for the deuteron energy range (1-8) GeV. In measurements with a lead blanket the absolute amount of produced ^{239}Pu nuclei increased by about 50% but staying constant in studied deuteron energy range, while the numbers of fissions remained virtually unchanged. The group analysis of DN time spectra indicates a growth in the average energy of the neutrons initiating fission of target nuclei from 15 to ~ 40 MeV with an increase in energy of the incident deuterons from 1 to 8 GeV. This result should be verified by experiments planned at the end of 2012.

*XXI International Baldin Seminar on High Energy Physics Problems
September 10-15, 2012
JINR, Dubna, Russia*

1. Introduction

The problems of global world power can not be apparently solved without the contribution of atomic energy. But the development of traditional nuclear power rests on the lack of resources commonly used fuel (plutonium or enriched uranium) and the key problem of utilization of radioactive waste (RAW). Recent decades as a perspective way to solve the RAW problem more seriously considered Accelerator Driven Systems (ADS). State ADS programs have been adopted in Europe, China and India.. The most striking example is the project MYRRHA [2], already running in Belgium

The main features of new promising ADS project aiming to recycle spent nuclear fuel (SNF) with simultaneous producing energy were presented during the last XX Baldin Seminar [1]. This project is based on so called Relativistic Nuclear Technology (RNT) proposed recently [3] by one of the institutions (CPTP «Atomenergomash», Moscow) participating collaboration.

Main physical idea of this approach is to use deep subcritical and quasi infinite (with negligible neutron leakage) multiplying target of natural (depleted) uranium or thorium combined with (5 – 10) GeV proton or deuteron incident beam. In accordance with some known experimental results and semi-phenomenological estimations [3] such ADS can provide extremely hard neutron spectrum within the active core (AC) and ensure an effective burning of core material as well as spent nuclear fuel (SNF) added to the initial core without its preliminary radiochemical reprocessing. To preserve hard neutron spectrum it is necessary to use helium gas cooling of the first circuit and core material as target for incident beam. Such ADS could have large enough beam power gain and produce additional energy in parallel with SNF utilization.

As for any ADS a necessary and key element is creation and use of powerful (~ 10-20 MW) accelerator with good enough duty cycle. It is proposed to utilize an original Russian technology BWLAC [4] for creation of reliable and compact MW linac.

All RNT engineering problems including creation of necessary accelerator have to be discussed practically after detailed study and verification of basic physics ideas of proposed approach.

This is just an aim of JINR project “Energy and Transmutation Radioactive Wastes” (“E&T RAW”) adopted for realization during 2011-2013 on the basis deuteron and proton beams of NUCLOTRON in incident energy range (1- 10) GeV and natural (depleted) massive uranium targets available at JINR.

The main goals of (E&T RAW) project are to study the basis characteristics of neutron fields inside deep subcritical quasi-infinite AC made of depleted uranium metal, the spatial distributions of core nuclei fission, the production of ^{239}Pu nuclei, the transmutation reaction rates of long lived minor actinides and fission products as well as to define optimal energy of incident beam for transmutation RAW and energy production.

2. Motivation

It is appropriate to note that ADS with quasi-infinite subcritical AC from natural or depleted uranium were studied earlier in papers [5-8]. In Ref. [5] there was studied AC made of natural uranium metal with mass ~19.5 t irradiated by 14 MeV neutron source located in the center of pile. (See Fig.1). Authors had measured the spatial distributions of neutron flux and many reaction rates inside of the pile. The results are shown in Fig.2. It is seen that energy neutron spectrum becomes essentially softer with increasing distance from the center of AC and neutron capture increases accordingly.



Figure 1: General view of the ADS assembly [5] showing the 99 cm diameter and 107 cm height pile. The effective uranium density is $\rho = 16.3 \text{ g/cm}^3$.

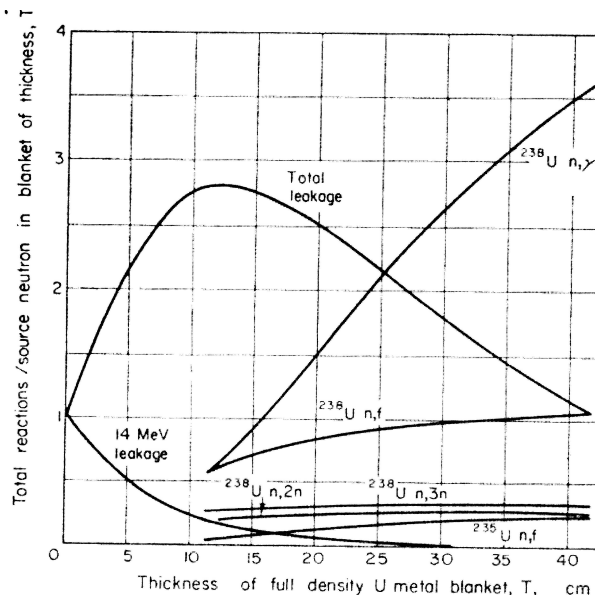


Figure 2: Results of measurements [5] of (n,γ)-, (n,f)-,(n,2n) and (n,3n)-reactions on ^{238}U nuclei, (n,f)-reaction on ^{235}U and neutron leakage.

The similar ADS setup had been studied in paper [6]. But this paper is not available. The main results obtained in Ref. [6] and some information about the respective setup is cited in [9]. As it follows from [9] the radius of AC used in [6] was 51 cm, the effective density of ^{238}U nuclei was 18.8 g/cm^3 and the admixture of ^{235}U isotope was 0.4154 %. The $^{238}\text{U}(n,f)$ -reaction rate only measured in Ref. [6] was 0.115 ± 0.052 per one source neutron whereas the corresponding result of Ref. [5] was 0.281 ± 0.017 with the concentration of ^{235}U isotope 0.72 %. The calculations of (n,f)-reaction rates on ^{238}U and ^{235}U isotopes made in Ref. [9] with use of different nuclear data libraries showed a satisfactory (within ~20%) agreement with experimental data [5,6]. But for wide neutron spectrum with energies up to hundreds of MeV, which is formed within the extended multiplying target under irradiation of high-energy particles a picture of processes within AC becomes much more complex.

In the experiment of C. Rubbia group [7] the “quasi-infinite” active core shown in Fig.3 was irradiated by protons with energies (0.6 – 2.75) GeV.

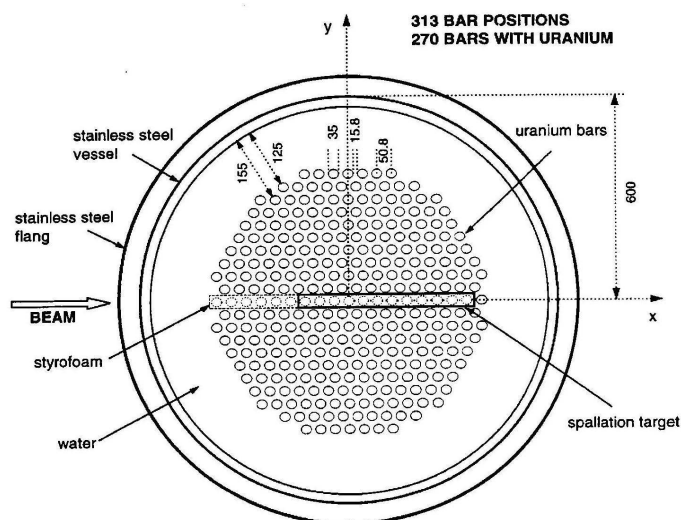


Figure 3: Top view of the FEAT subcritical assembly. The picture is from Ref. [7], sizes in mm.

It is necessary to note that in experiment [7] the natural uranium pile of total mass ~ 3.5 t was loaded in a water tank so produced neutron spectrum was practically the thermal one. The value of $k_{eff} \approx 0.9$ measured in [7] indicates that the fission rate in this AC defines mainly by admixture of ^{235}U isotope. So the basic result of Ref. [7] shown in Fig. 4 namely a constant value of beam power gain (BPG ≈ 30) above $E_p > 1 \text{ GeV}$ normalized to one incident proton is associated with an impurity of ^{235}U nuclei too. In these circumstances in spite of rather promising BPG it is difficult to implement "burning" of the base core nuclei because of their high fission threshold. And actually proposed C. Rubbia's idea of Energy Amplifier must move on to the enriched fuel.

Most interesting and close to the (E&T RAW) project is experiment [8] performed

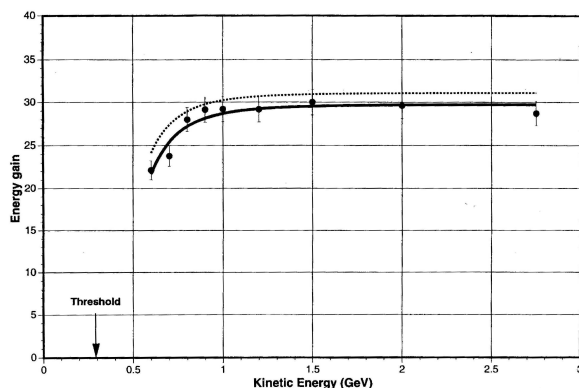


Figure 4: Beam power gain in dependence on incident proton energy (the picture from [7]).

at JINR synchrocyclotron with proton beam energy range (0.3 - 0.66) GeV. In this experiment there was used the deep subcritical target assembly presented in Fig. 5. It consisted of about three tons of metallic natural or depleted uranium and 10 cm lead blanket. Due to the special geometry of an asymmetric beam input the results obtained in such way were equivalent to the same for the axisymmetric target mass of ~ 7 tons. There was no any dedicated moderator and the neutron leakage from the target assembly as estimated by authors was ~10%. So unlike Ref. [7] in this case has been realized an extremely hard neutron spectrum.

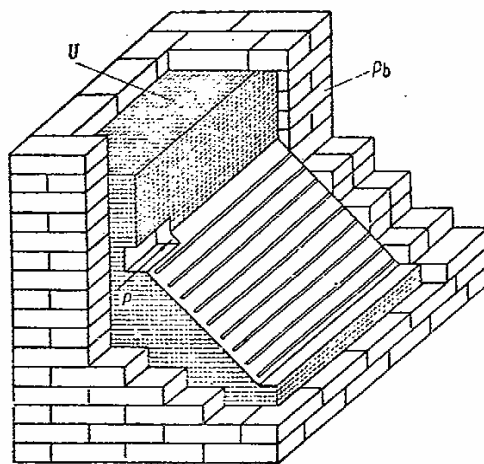


Figure 5: Target assembly of experiment [8]. Dimensions of uranium target 56x56x64cm.

The total numbers of fission in the equivalent target assembly obtained by integration over the measured spatial distributions of fission rates at 660MeV proton energy were 13.7 ± 1.2 and 18.5 ± 1.7 per one incident particle for depleted and natural uranium, respectively. According to the authors [8], it was not accounted for 3-4 fission events (per one proton) occurring in the cascade region of the central zone of the target with a diameter of 10 cm due to specific design

of the experimental setup. Thus, the beam power gain for this proton energy could be estimated (see [1] for more detail) as ~ 6.0 and ~ 7.4 for depleted and natural uranium, respectively. It is necessary to mention one more result obtained in Ref. [8]. When uranium in the center of the target was replaced with lead core with dimensions 8×8 cm the total neutron multiplicity and accordingly total fission yield decreased approximately twice. Thus the use of core material as a target for incident beam as it is adopted in RNT approach provides significant benefit.

So it is very attractive to investigate such type of ADS for higher incident energy discussed in the frame of RNT concept. At JINR there are very favorable conditions for realization such research. Here is the suitable accelerator NUCLOTRON with deuteron and proton beams to energy of 5 GeV per nucleon. Beside that there is available the extended natural uranium metal (500 kg, $\phi 30$ cm x 65cm) target assembly (TA) QUINTA and the quasi-infinite depleted uranium metal (19.5t, $\phi 120$ cm x 100cm) target setup BURAN (an Russian abbreviation – Large Uranium target) shown in Fig. 6 and 7 below.



Figure 6:. General view of target assembly QUINTA.

The construction of QUINTA TA is described in more detail in the next section. Here it is important to note that basic aim of all measurements with this target is to prepare and to test the experimental technique for realization of main research program with BURAN setup. Of course, the results obtained in experiments with QUINTA TA and presented below have independent meaning for understanding and modeling the processes occurring in the central zone of BURAN setup.

The design of BURAN setup is shown in Fig. 7. It has a steel case, the replaceable central zone diameter of 20 cm and many axial detector channels are shown in red. The frame provides a precise positioning of the target. In general BURAN setup is well suited for realization of extended research program adopted in the “E&T RAW” project for 2013-2014.. But it requires more design and experimental methodology work to launch in 2013 a research program with BURAN setup briefly outlined by the end of Introduction above.

Below an overview of the results of experiments carried out with QUINTA TA during 2011-2012 aimed at study basic features of RNT is presented.

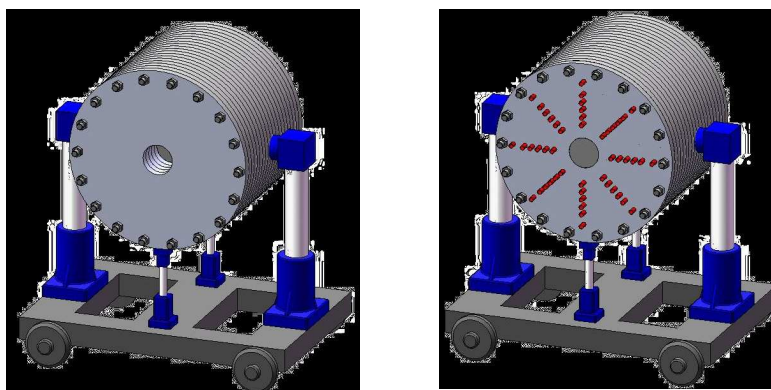


Figure 7: Front and rear view of target setup BURAN (left and right pictures respectively).

3. Experiment

During three last NUCLOTRON runs (March 2011, December 2011 and March 2012) the target assembly QUINTA was irradiated by deuterons with energies of 2, 4 and 6 GeV in the first above mentioned run and of 1, 4 and 8 GeV in the other two. The scheme of experiments is presented in Fig. 8.

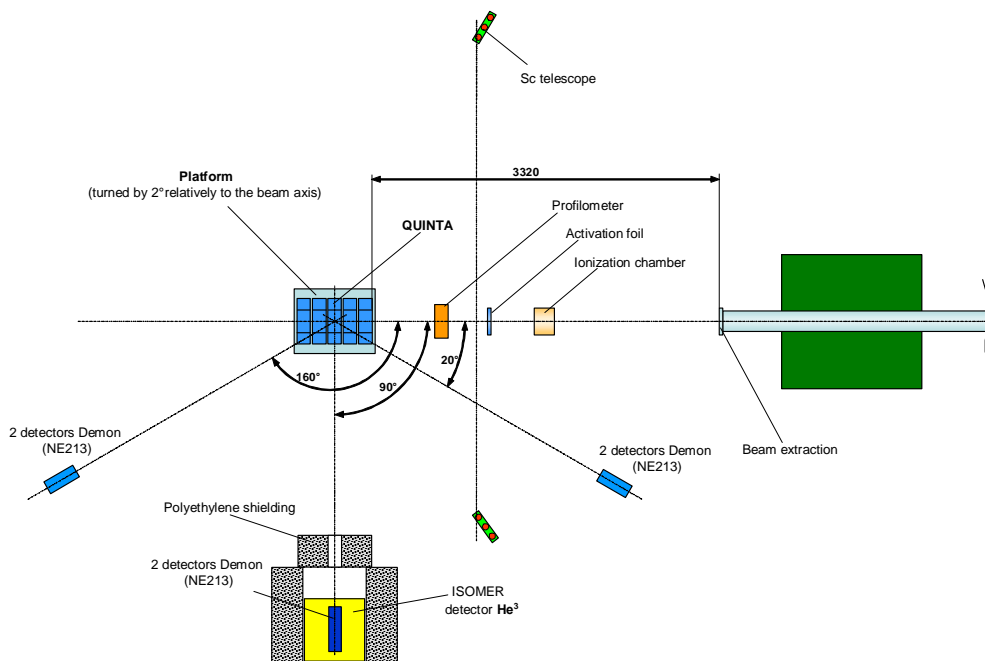


Figure 8: The scheme of experiments with QUINTA target assembly.

The extracted pulsed deuteron beam of the JINR NUCLOTRON [10] hits the target from the exit window located on it in 3.32 m. The spatial and time profile, as well as an intensity of

each deuteron pulse were monitored using calibrated and position sensitive ionization chambers in coincidence with two scintillation telescopes. The beam position on the target and the integral deuteron flux were controlled by the profilometer and activation monitors from aluminum foil and solid state track detectors placed before the target. Prompt neutrons were measured by the detector DEMON with the liquid scintillator NE213 inside. This detector has a large (~ 30%) efficiency for neutrons of high (up to 100 MeV) of energy. Delayed neutrons (DN) were recorded by the detector system ISOMER-M [11]. It consists of 11 proportional ³He- counters placed into the 50 x 50 x 60 cm Plexiglas moderator block. Each counter was equipped with the preamplifier and discriminator. The ISOMER-M efficiency for registration of neutrons from the Pu-Be-source with the average spectrum energy of 4.4 MeV was 11.4±0.1%. The detector was surrounded by appropriate shielding from borated polyethylene. The DAQ system provided measurement of the neutron yield as a function of time for each deuteron pulse.

The target assembly QUINTA shown in Figs. 9 and 10 consists of four identical sections of hexagonal aluminum containers with an inscribed diameter of 284 mm, each of which is placed for 61 cylindrical uranium block. Blocks of 36 mm diameter and a length of 104 mm made of metallic natural uranium and placed in sealed aluminum housing. Unit weight is 1.72 kg and the total mass of uranium in one section is 104.92 kg. The front section has the cylindrical input beam channel diameter 8 cm. The total mass of uranium in the target assembly is close to 500 kg. In front of the target and between its sections as well as behind it there are 6 detector's plates. Connected to each other sections are fixed on aluminum plate and placed on a mobile carriage allows for precise adjustment of the axis of the target relative to the direction of the incident beam. To prevent the free passage of the some part of incident beam through the horizontal space between the tightly packed uranium cylinder an axis of the target assembly set with the rotation of 2 degrees with respect to the beam axis.

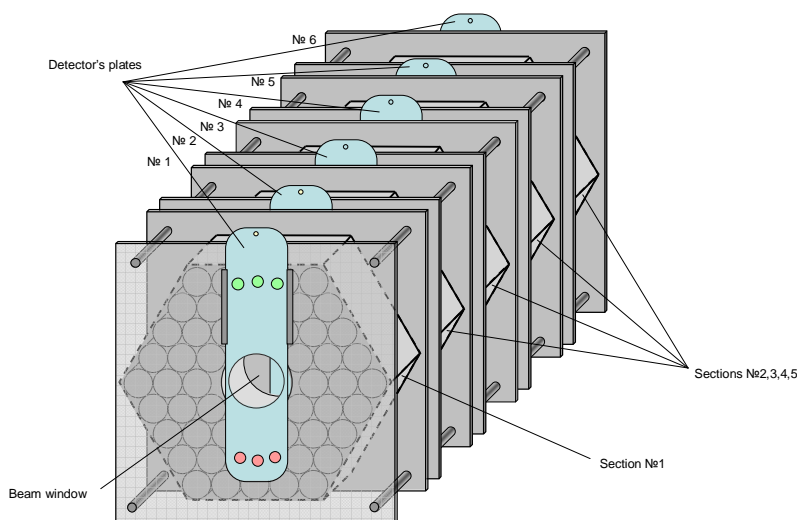


Figure 9: The layout of the target assembly QUINTA.

In experiments of December 2011 and March 2012 there was added to the uranium target the lead blanket thickness of 10 cm with the input beam window size of the 150x150 mm shown in Fig.10. In the top cover blanket was made special slots with lids for quick removal of detector's plates.

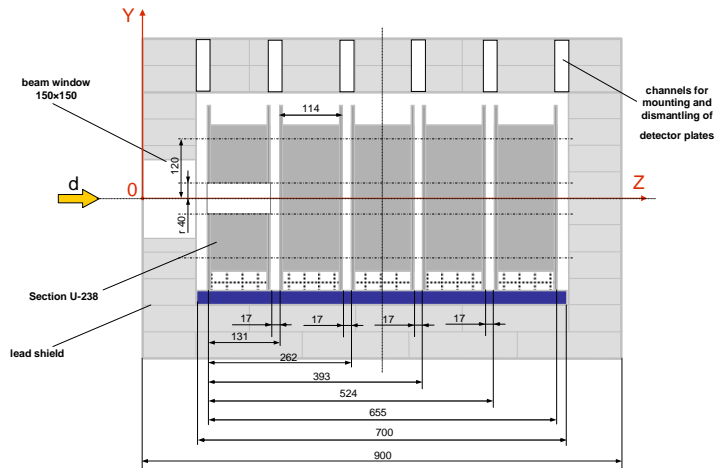


Figure 10: The cross cut of target assembly QUINTA equipped by lead blanket. Sizes are in mm.

The general view of whole experimental setup placed at the focus #3 of NUCLOTRON beam is shown in Fig. 11. In the foreground are seen two ionization chambers designed for on-line monitoring of the beam intensity. The control room is located ~ 30 meters from the target.



Figure 11: General view of experimental setup.

3.1 Monitoring of beam intensity.

The total beam intensity was determined in parallel by three independent groups with aid of the activation analysis method using ^{27}Al foils. Other activation materials could not be used

due to missing cross-sections or improper gamma-ray properties and half-lives. Aluminum foils for the beam intensity measurement were placed in different places between the beam tube window and the target. In the process of irradiation, stable isotope ^{27}Al was transmuted by (d,3p2n) reaction into radioactive ^{24}Na isotope. The yield (i.e., the number of nuclei activated in the foil during the whole period of the irradiation) of produced gamma-radioactive nuclei was determined using gamma-spectroscopy. The method of obtaining the absolute yield of ^{24}Na isotope is described below in some detail on example of the data obtained during March 2012 run by Řež group.

Original dimensions of the foils were $10 \times 10 \times 0.0196 \text{ cm}^3$. After irradiation, the each foil was packed into a smaller one with dimensions approximately $2.5 \times 2.5 \times 0.3 \text{ cm}^3$ for the spectroscopy measurements. Activated foils were measured on three HP Ge detectors, in two different geometries marked p2 and p5 which were 2.4 and 9.9 cm far from the (B) detector and in two different geometries marked p2 and p5 which were 2.4 and 9.9 cm far from the (C) detector and in geometry marked p2 which was 2.4 cm from the (E) detector. The detectors were calibrated using standard laboratory ^{54}Mn , ^{57}Co , ^{60}Co , ^{109}Cd , ^{133}Ba , ^{137}Cs , ^{152}Eu , ^{228}Th , and ^{241}Am point sources which have several gamma-lines ranging from 60 keV up to 2610 keV. Evaluated calibration activities include correction on real coincidences for isotopes with more lines. Total number of points used for one calibration curve is more than 35. Calibration curves are third order polynomials divided into two parts, one for lower energies and one for higher energies. The typical calibration curves for the used detectors are presented in Fig. 12.

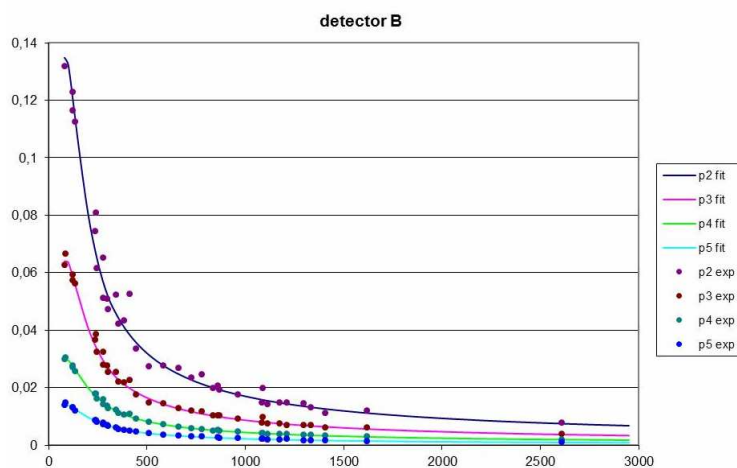


Figure 12: Efficiency curves for detector (B) (the abscissa – γ -line energy keV, the ordinate – an efficiency). Peak efficiency fit is in solid line.

Gamma-spectra were evaluated in the Deimos 32 code [12]. From the gauss-fit of the peaks we got also the statistical uncertainty (any other uncertainties were not taken into account in following evaluation). Total yield of ^{24}Na in the aluminum foil was determined according to the next equation (1) (all corrections were included, for details see [13]):

$$N_{yield} = \frac{S_p \cdot C_{abs}(E) \cdot B_a}{I_\gamma \cdot \epsilon_P(E) \cdot C_g \cdot C_{area} \cdot C_{live} \cdot C_{dead} \cdot C_{cool}} \cdot e^{\lambda t_0} \cdot \frac{\lambda \cdot t_{irr}}{1 - e^{-\lambda t_{irr}}}$$

(1)

where: λ is decay constant, t_{irr} – irradiation time, t_{real} – real measurement time, t_{live} – live time of the detector, t_0 – cooling time.

To get beam intensity as precise as possible, various spectroscopic corrections shown in equation (1) were applied.

3.1.1 Correction on beam intensity changes during irradiation (B_a)

Really the beam intensity was changing during deuteron irradiations. As example of the time scenario of March 2012 run for deuteron energy 8 GeV measured on-line by ionization chambers is shown in Fig. 13.

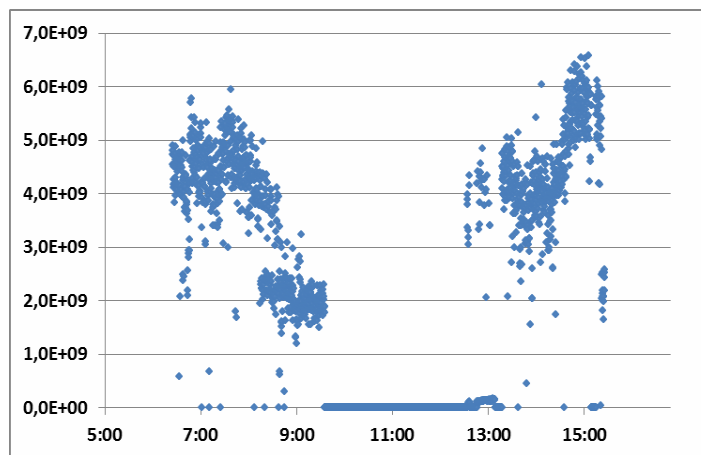


Figure 13: The time dependence of deuteron beam intensity during irradiation of QUINTA TA at the energy 8 GeV. Time is given in hours.

The code [14] was used to calculate the correction value B_a by formula (2). This code calculates a shapeless number according to the equation (2), every bunch is taken as one interval.

$$B_a = \frac{1 - e^{-\lambda_{irr}}}{t_{irr} \sum_{i=1}^N \left[\frac{1}{t_p(i)} W(i) e^{-\lambda_e(i)} (1 - e^{-\lambda_p(i)}) \right]} \quad (2)$$

Here: t_{irr} is the total irradiation time, $t_e(i)$ – time from the end of the irradiation interval till the end of the whole irradiation, $t_p(i)$ – time of calculated irradiation interval, $W(i)$ – ratio between the number of deuterons in the interval i and in the whole irradiation, N – the total number of intervals. The results are given in Table 1.

Table 1: Beam instability correction factors for ^{24}Na .

Deuteron energy [GeV]	$T_{1/2}$ [h]	Correction factor B_a
1	14.959	1.00208
4		1.00886
8		1.00140

3.1.2 Correction on non-point like emitters (C_{area})

The HPGc detectors were calibrated with point-like laboratory etalons, so the calibration is in close geometries valid only for point sources. The aluminum samples could not be measured far enough from the detector due to their low activity, so the correction on non-point like emitters has to be taken into account. It has been done with aid of MCNPX simulation, in which response of the detector on point-like and non-point like emitter is studied, see equation (3). Correction values in the case of $2.5 \times 2.5 \times 0.3 \text{ cm}^3$ emitter are summarized in Table 2. Correction was verified in multiple experiments, for more details see [15].

$$C_{area} = \frac{\epsilon_p(\text{foil})}{\epsilon_p(\text{point})} \quad (3)$$

Table 2: Correction factors on non-point like emitters, detector A, B, C and E.

Position	Detector A	Detector B	Detector C	Detector E
p2	0.957	0.963	0.963	0.963
p5	0.994	0.992	0.992	0.992

3.1.3 Correction on self-absorption (C_{abs}) and due to sample dimensions (C_g)

The aluminum foils have after the folding from $10 \times 10 \text{ cm}^2$ onto $2.5 \times 2.5 \text{ cm}^2$ thickness approximately 3 mm, so the self absorption of the ^{24}Na gamma photons could not be neglected. The respective corrections were calculated according to the equation (4), Quantity μ standing in the integrand is the total mass attenuation coefficient μ_T [g/cm^2] divided by density ρ [g/cm^3]. The coefficient μ_T comes from the text book [16].

$$C_{abs} = \frac{\int_0^D \frac{I_0}{D} dx}{\int_0^D \frac{I_0}{D} e^{-\mu \cdot x} dx} = \frac{\mu \cdot D}{1 - e^{-\mu \cdot D}} \quad (4)$$

The obtained correction factors were 1.021 for 1368 keV gamma line and respectively 1.015 for 2754 keV one.

The small corrections C_g on changed detector efficiency had to be included related to the sample positions during measurement. The 3 mm thick foil had its centre approximately 1 mm closer to the detector than was the position for which the calibration was done. Detector efficiencies were taken for positions p2-p5 and a curve was fitted through them. Then the detector efficiency for position 1 mm closer to the detector was calculated. Ratio of the new and original efficiency is the searched corrections (1.042 for 1368 keV, 1.039 for 2754 keV). These are approximately the same for all used geometries

3.1.4 Beam intensity calculation

The value of the integral deuteron flux at each incident energy can be calculated by next formula:

$$N_d = \frac{N_{yield} \cdot S \cdot A}{\sigma \cdot m \cdot N_A} \quad (5)$$

where N_{yield} is the total amount of produced ^{24}Na nuclei, A – molar weight, σ – the cross-section of $^{27}\text{Al}(d,3p2n)^{24}\text{Na}$ reaction, m – weight of the foil, S – its area, N_A – Avogadro's number.

Following the procedures described above one can determine the value of N_d using the known cross-section $\sigma(E_d)$. Unfortunately, there are known only three experimental values of the cross-sections for $^{27}\text{Al}(d,3p2n)^{24}\text{Na}$ reaction in the GeV energy range. The one of Ref. [17] is $(15.25 \pm 1.5 \text{ mb})$ at 2330 MeV and two other are from Ref. [18] - $(14.1 \pm 1.3 \text{ mb})$ at 6000 MeV and $(14.7 \pm 1.2 \text{ mb})$ at 7300 MeV, see Fig. 14.

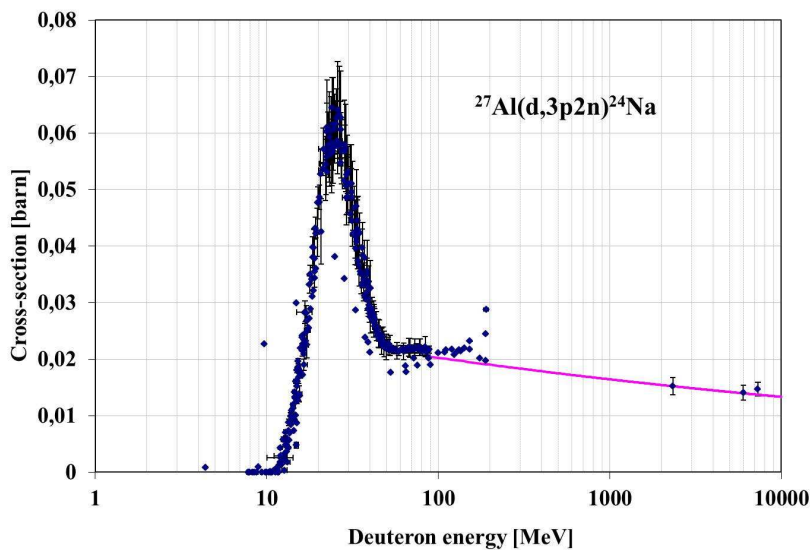


Figure 14: Cross-section of $^{27}\text{Al}(d,3p2n)^{24}\text{Na}$ reaction – experimental data and fit of the points.

The fit of experimental data in the energy range (0.1 – 7) GeV by function $\sigma = a \cdot E^b$ (linear in log scale of energy) allows one to obtain the interpolated values of the $^{27}\text{Al}(d,3p2n)^{24}\text{Na}$ reaction cross-sections for all deuteron energies used in our experiments. The estimated uncertainties are about 10%. The respective values are presented in Table 3 for deuteron energies realized in our measurements.

Table 3: Interpolated cross-sections of $^{27}\text{Al}(d,3p2n)^{24}\text{Na}$ reaction.

Deuteron energy [GeV]	Cross-section [mb]	Estimated uncertainty [mb]
1.0	16.4	1.6
2.0	15.4	1.5
4.0	14.5	1.5
6.0	14.0	1.4
8.0	13.6	1.4

These cross-sections were used below for absolute normalization of monitoring data.

To obtain the yield of ^{24}Na nuclei N_{yield} gained at given beam energy a set of measurements of the gamma lines 1368 and 2754 keV were realized and a weighted average was calculated together with its uncertainty. The set of integral deuteron fluxes obtained in accordance with such procedure are shown in Fig. 15 for measuring at deuteron energy of 1 GeV in March 2012.

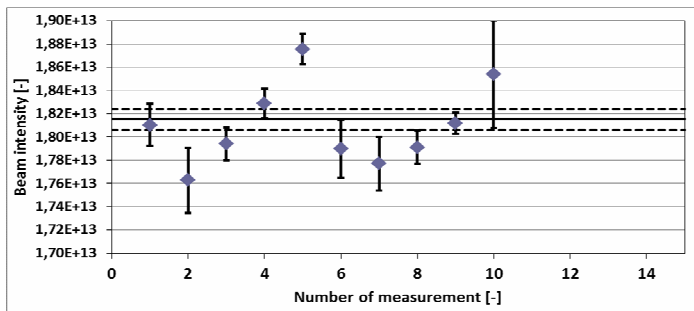


Figure 15: Measured beam intensities and its weighted average obtained for 1 GeV deuteron energy in March 2012 (first five points belong to the gamma-line 1368 keV and the rest ones - to 2754 keV line).

In Table 4 there are presented the integral deuteron fluxes for all three runs obtained independently by different experimental groups of the collaboration. The uncertainties of efficiency and spectroscopic corrections were very similar to all three groups. Their values are about (4 – 5) %. The errors in Table 4 include the sum of statistical uncertainties as well as errors of the mentioned efficiencies and other corrections discussed above. These were calculated by each group independently. A rather good agreement between results of different

Table 4. The integral deuteron fluxes for all three runs

Run	Energy [GeV]	Řež group [10^{13}]	Dubna group [10^{13}]	Khar'kov group [10^{13}]	Weighted mean value [10^{13}]
March 2011	2	1.69(8)·	1.42(9)·	1.40(14)·	*1.69(8)·
	4	1.41(7)·	1.29(8)·	1.40(14)·	*1.41(7)·
	6	1.94(10)·		1.70(17)	*1.94(10)·
December 2011	1	1.47(6)·	1.53(11)·	1.47(5)·	1.50(4)·
	4	1.93(8)·	1.78(16)·	1.96(6)·	1.94(5)·
	8			**0.063	
March 2012	1	1.82(8)·	1.88(8)·	1.90(11)·	1.86(5)·
	4	2.79(11)·	2.65(12)·	2.72(15)·	2.72(7)·
	8	0.556(25)·	0.536(24)·	0.37(8)·	0.539(17)

*These values are taken from the results of Řež group as most accurate and confident in comparison with other ones.

**The value is measured by an ionization chamber only.

groups is observed. Only exception is measurement of Khar'kov group for 8 GeV in March 2012 run. To take into account this discrepancy their uncertainty was increased in that individual case.

The beam intensities from Table 4 were used below for the normalization of the data discussed. But, of course, the systematic errors related to the uncertainties of $^{27}\text{Al}(d,3p2n)^{24}\text{Na}$

reaction cross-sections listed in Table 3 must be taken into account additionally for all observable values.

3.2. Measurements of spatial distributions of fission rates and ^{239}Pu nuclei production

In all three runs there were measured the spatial distributions of the fission rate and ^{239}Pu isotope production. The fission rates were studied with aid of activation technique [19] and solid state track detectors (SSTD) [20].

The activation samples in shape of natural uranium disks (diameter 10 mm and thickness 1mm) were situated on all six detector plates in the range of radii as it is shown in Fig.16. The red circles marked the location of samples with a unit corresponds to the beam axis, the numbers 2, 3 and 4 indicate $r = 40, 80$ and 120 mm respectively below the axis and 5 – $r = 80$ mm above the axis.

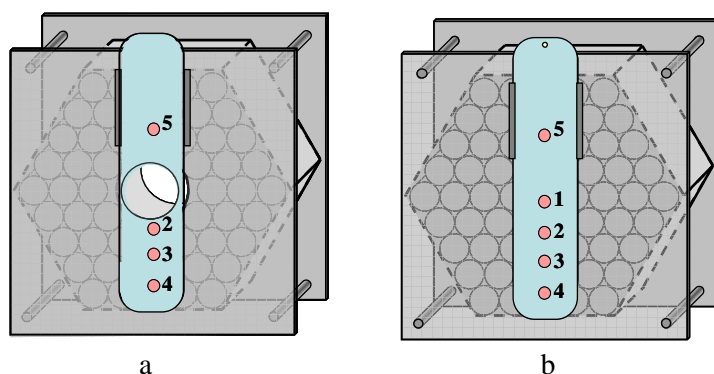


Figure 16: Location of activation samples on the plates, (a) shows the entrance one and (b) – all other.

It is assumed that fission in QUINTA TA is related mainly with ^{238}U and induced by neutrons formed under irradiation of deuteron beam. Fission related with high energy deuterons has small cross-section and is not included in the consideration. A selection of specific fission products (FP) is determined by the fact that their yields vary little over a wide range of neutron energies. From measurements of γ -spectra of irradiated uranium samples the yields of specific FP have been obtained. The procedure of extraction of FP yields was the same as described above in Section 3.1. The numbers of ^{238}U fissions at each position inside of QUINTA TA were obtained by averaging of following FP yields: ^{97}Zr (5.42%), ^{131}I (3.64%), ^{133}I (6.39%), ^{143}Ce (4.26%) known from literature. In brackets the cumulative yields of respective FPs averaged over data for neutron energy range (2-22) MeV are shown. The density distributions of fission numbers N_f normalized per gram of uranium, per one deuteron and per 1 GeV are shown conditionally in Fig. 17. The curves are drawn by eye for convenience of comparison of results obtained in different cycles. The first digits in the numbers of standing next to the curves indicate the number of detector plates. The meaning of second digits explained above.

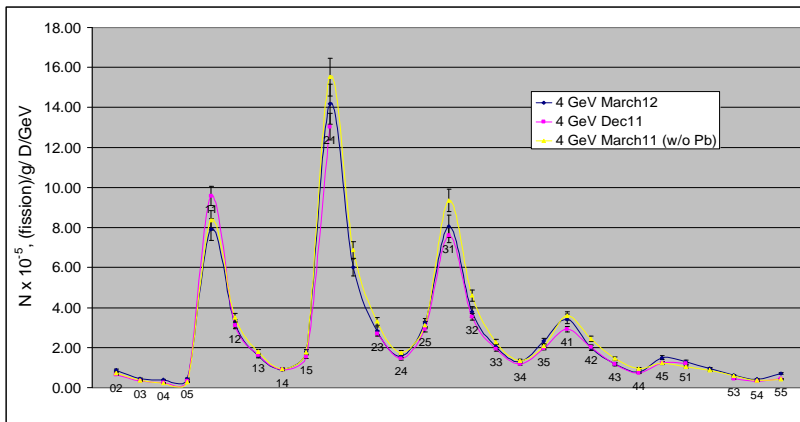
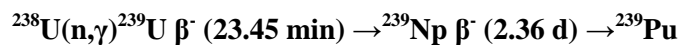


Figure 17: Density distribution of the ^{238}U fission numbers N_f measured at deuteron energy of 4 GeV in three runs (yellow – March 2011, red – December 2011 and black – March 2012).

It is seen that an addition of the lead blanket does not change practically measured spatial distribution of fission rates.

The same uranium samples were used for study of the ^{239}Pu isotope production going through neutron radiative capture by the ^{238}U nuclei within QUINTA TA. The respective chain of nuclear transformations is presented below.



Before measurement the irradiated uranium samples were exposure for more than 4 hours to reach 99.9% of the ^{239}U nuclei decay. The number of the produced ^{239}Pu nuclei N_{Pu} was determined [19] by measuring the activity of the ^{239}Np nuclides.

The obtained density distributions of the N_{Pu} numbers are represented in Fig.18 in the

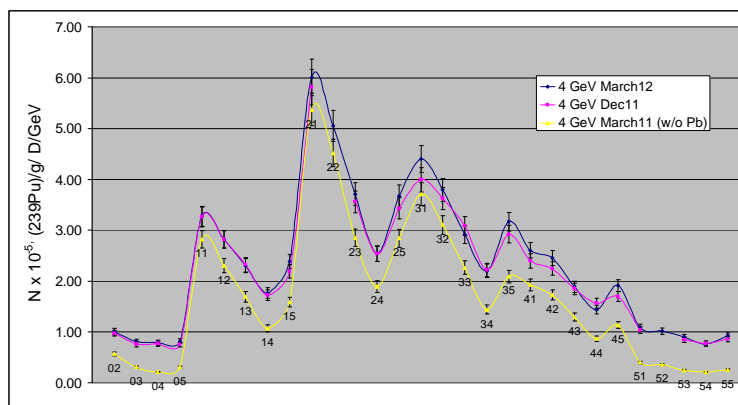


Figure 18: Density distribution of the ^{239}Pu isotope production numbers N_{Pu} measured at deuteron energy of 4 GeV in three runs (yellow – March 2011, red – December 2011 and black – March 2012).

same normalization and in similar form as in Fig. 17. In contrary with fission there was observed about 50% increase when the lead blanket has been added (see yellow curve).

The radial and axial dependences of the N_f and N_{Pu} numbers at different deuteron energies measured in March 2012 run are given in Fig. 19. All data is normalized as in Fig. 17 and 18. The obtained results show a visible dependence on the deuteron energy a behavior of the radial distributions at different distances along beam axis. An especially strong effect is seen at the entrance to the target ($Z = 0$).

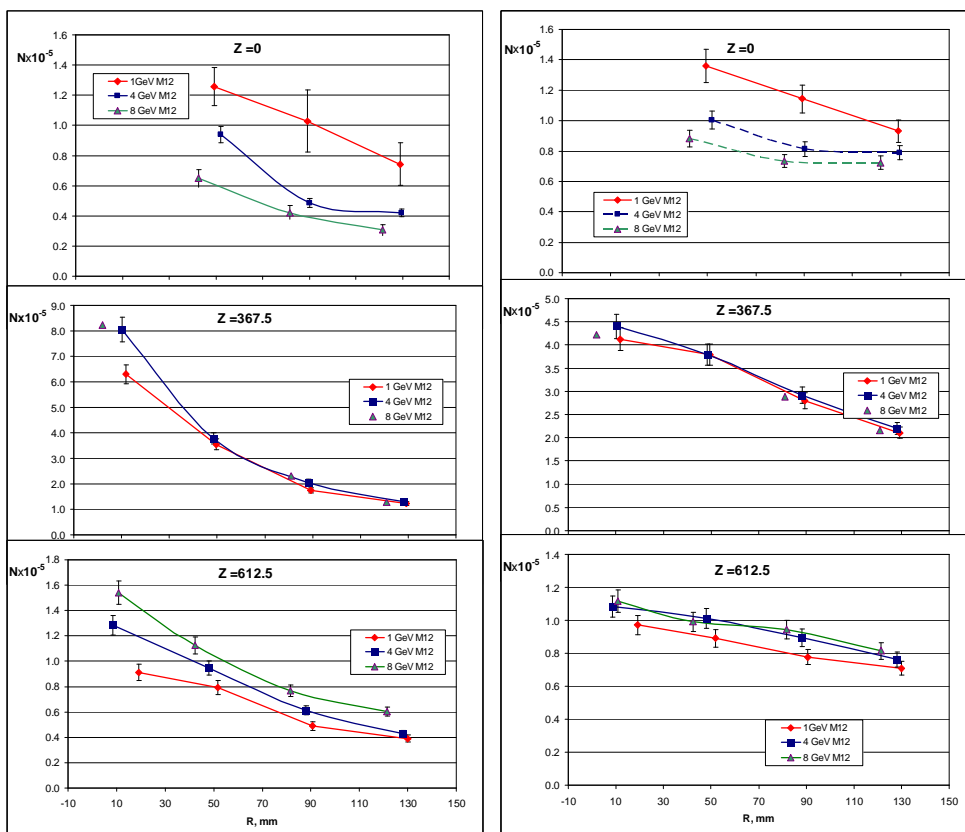
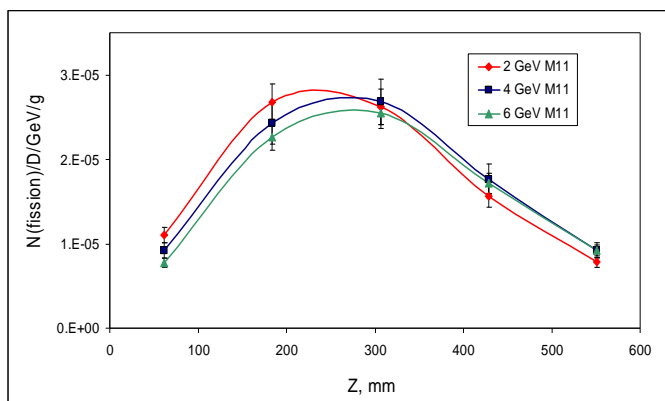


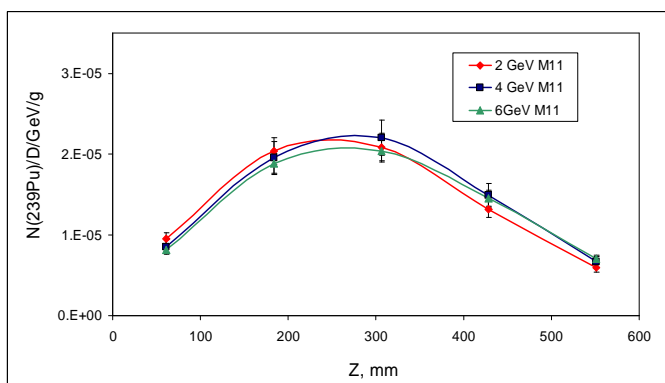
Figure 19: Radial distributions of density of the N_f and N_{Pu} numbers (left and right side of the figure) measured in March 2012 at deuteron energies 1, 4 and 8 GeV (the legends are in inserts).

The axial dependence of the N_f and N_{Pu} values averaged over radial cross sections of TA as well as their ratios N_{Pu} / N_f , so called spectral indices measured in March 2011 are presented in Fig. 20 with the same normalization as previously. There is good agreement between the obtained axial distributions for all deuteron energies. In the middle of TA the spectral indices are practically constant. But in first section of TA it increases by about 30% and falls slightly in the last one. The effect of lead blanket on average axial distributions of the N_f , N_{Pu} and spectral

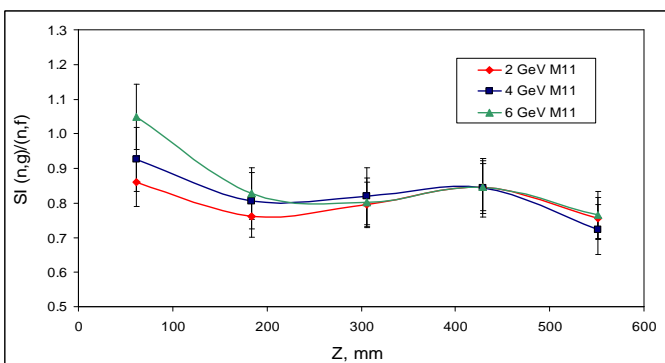
indices is demonstrated in Fig. 21. A comparison of data obtained in March 2011 and 2012 shows a preservation of the N_f number distributions, an essential change of the N_{Pu} values and,



a



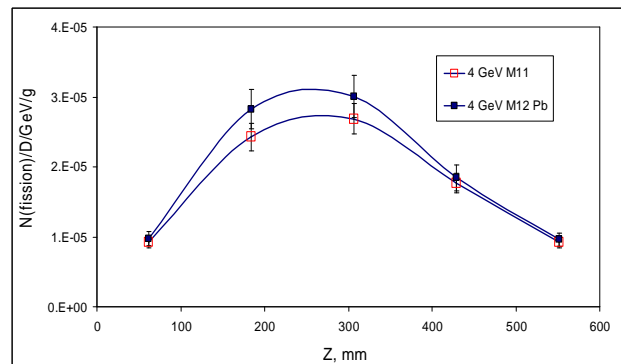
b



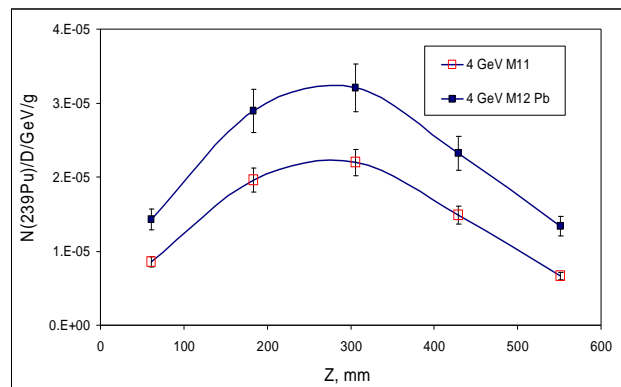
c

Figure 20: Axial density distributions of the N_f , N_{Pu} and spectral indices (a, b and c accordingly) averaged over the respective radial distributions (measurements March 2011).

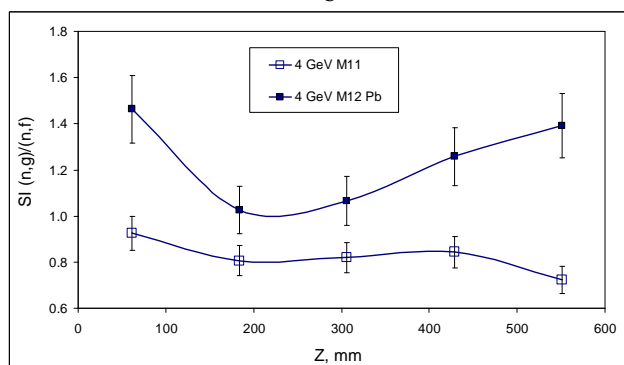
respectively, the average spectral indices. An increase of these indices shows a marked softening of the neutron spectrum inside the target assembly by adding the lead blanket.



a



b



c

Figure 21: Comparison of the average axial distributions of the N_f , N_{Pu} and spectral indices measured at deuteron energy of 4 GeV in March 2011 and 2012 (a, b and c accordingly).

For measurement of fission rates by SSTD the similar uranium samples were used as in described above. The sandwiches of uranium disks and track detectors were located on the same

plates in five symmetrical positions as it is shown in Fig. 22. The spatial distributions of fission rates were measured and processed by the method described in Ref. [20].

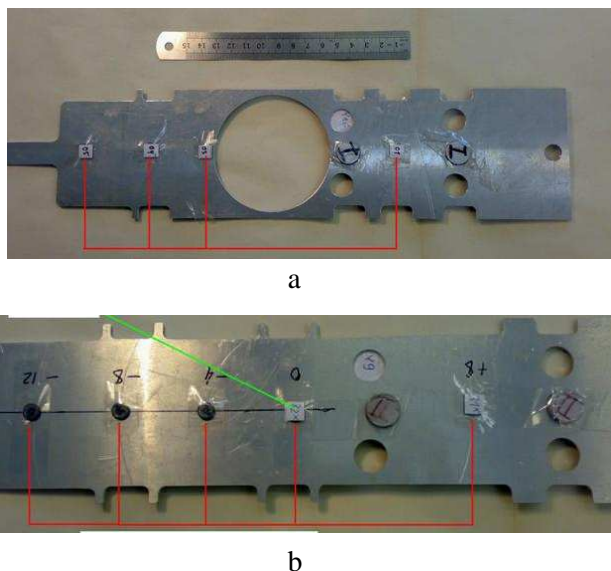


Figure 22: Location of SSTD on detector plates, (a) is the entrance one and (b) – all other.

A typical example of results is given in Fig. 23. Here are a two dimensional (in plane YZ, see Fig.10) distributions of fission numbers per one cm³ and one deuteron measured in March 2012 at incident energies of 1, 4 and 8 GeV.

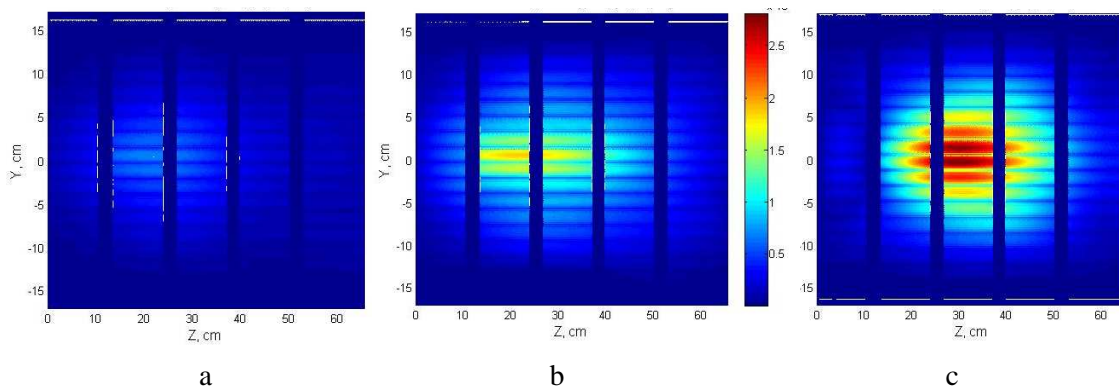


Figure 23: Two dimensional distributions of fission numbers per one cm³ and one deuteron measured in March 2012 at incident energies of 1, 4 and 8 GeV (a, b and c respectively).

In these figures it is clear that with increasing of deuteron energy is rapidly expanding a volume of the domain inside the multiplying target where fission is effective. So there is some potential for enhancement of beam power gain with increase of the size of AC.

3.3 Calculation of total numbers of fission and the produced ^{239}Pu nuclei

By integration over TA volume the measured spatial distributions of fission numbers and of the amounts of the ^{239}Pu nuclei formed the total values of the respective numbers could be obtained. But doing this must be considered the exact geometry of the experiment, namely, the difference in the actual state of the beam axis and the axis of the target. In measurement for a given energy the target axis is set as closely as possible with respect to the geometrical axis of the output beam channel and as mentioned above is rotated by 2 degrees. In reality, during beam extraction its direction can be different from the ideal. In each measurement there was carried out monitoring the position and shape of the beam at the target with aid of SSTD. The results of all such measurements are summarized in Table 5. (more details see in Ref. [21]).

Table 5. Deuterons beam parameters measured in March 2011, December 2011 and March 2012 runs.

Run	Deuteron energy, GeV	Coordinates of beam center, cm		FWHM of beam shape, cm	
		X_c	Y_c	FWHM_x	FWHM_y
March 2011	2	1.2	-0.5	2	2.8
	4	1.2	-0.7	2.2	2.3
	6	2.0	-0.1	3.9	3.1
December 2011	1	1.3	0.2	2.6	3.5
	4	1.4	0.2	1.5	1.4
March 2012	1	0.6	0.9	2.9	3.2
	4	2.0	0.8	1.1	1.2
	8	1.2	0.10	0.9	1.2

Using the real geometry of each measurement the integration over volume of TA has been done and the results are given in Table 6.

As follows from Table 6 the values N_f^{tot} and N_{Pu}^{tot} are approximately constant in limit of their uncertainties at least up to the deuteron energy of 6 GeV. The data obtained for incident energy of 8 GeV need additional verification that should be done in December 2012 NUCLOTRON run. An effect of increasing in the total numbers N_{Pu}^{tot} by the inclusion of the lead blanket was about 50% slightly lower than for spatial distributions.

Table 6. The total numbers of fission (N_f^{tot}) and of the produced ^{239}Pu nuclei (N_{Pu}^{tot}) (in units of per one deuteron and 1 GeV)

Run	$E_d = 1$ GeV	$E_d = 2$ GeV	$E_d = 4$ GeV	$E_d = 6$ GeV	$E_d = 8$ GeV
SSTD method					
Total numbers of fissions N_f^{tot}					
03.11		11 ± 1.9	9.4 ± 1.7	9.6 ± 1.7	
12,11	11.8 ± 2.0		8.2 ± 1.5		10.0 ± 1.7
03.12	8.9 ± 1.5		8.1 ± 1.5		$*9.2 \pm 1.6$
Activation method					
Total numbers of fissions N_f^{tot}					
03.11		$(8.8 \pm 0.4) \pm 1.0$	$(8.8 \pm 0.4) \pm 1.0$	$(8.3 \pm 0.4) \pm 0.9$	
12,11	$(10.6 \pm 0.5) \pm 1.1$		$(8.5 \pm 0.4) \pm 1.0$		
03.12	$(10.5 \pm 0.5) \pm 1.1$		$(9.7 \pm 0.4) \pm 1.0$		$*(9.7 \pm 0.5) \pm 1.1$
Total numbers of the produced ^{239}Pu nuclei					
03.11		$(7.0 \pm 0.3) \pm 0.8$	$(7.2 \pm 0.4) \pm 0.8$	$(6.9 \pm 0.3) \pm 0.7$	
12,11	$(11.8 \pm 0.6) \pm 1.2$		$(10.8 \pm 0.5) \pm 1.1$		
03.12	$(11.6 \pm 0.6) \pm 1.2$		$(11.3 \pm 0.5) \pm 1.1$		$*(10.5 \pm 0.5) \pm 1.1$

* These values were obtained with the original Khar'kov group beam intensity (see Table 4). If one uses the weighted value of this intensity so respective numbers reduce by 30%.

3.4 Measurements of leakage neutrons

The time dependence of leakage neutron yields measured between NUCLOTRON bursts with aid of detector system ISOMER-M provides valuable information on fission processes within the target assembly [22]. The incident deuteron beam had duration of pulse ~ 500 ms with repetition rate ~ 8 s⁻¹. Really in time interval from ~ 1 to 7.5 s after a burst's start only source of neutrons could be delayed ones originated from fission of uranium nuclei. Fission in the lead blanket is negligible as shown in Ref.[22]. The time spectra of neutron yield (normalized to one incident particle) measured in course of irradiation of TA QUINTA in March 2011 at deuteron energy of $E_d = 6$ GeV is shown in Fig. 24. The time structure and intensity of deuteron burst were monitoring one-line for each accelerator pulse. Some details of the DN measurements were given above in the beginning of Section 3 (see also [11] and [22]). Special measurements showed that the contribution of the background to these spectra was negligible

The detailed analysis of the shape of DN time spectra allows one to obtain information on characteristics of precursors of delayed neutrons studied in experiments. Due to specific conditions of the performed experiments (the narrow time window for detection of DN) it is possible to get information only about the short-lived precursor groups. So a decomposition of

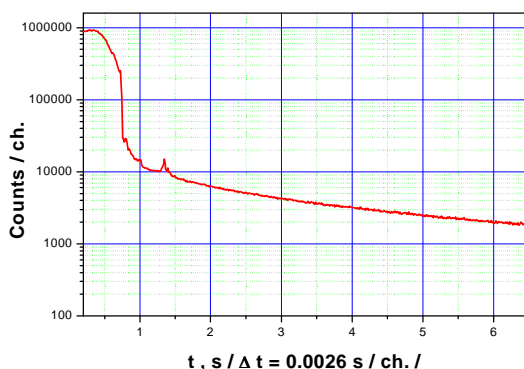


Figure 24: The time dependence of neutron leakage from TA QUINTA irradiated by 6 GeV deuterons.

the DN time spectra was made only accounting for the groups with half-life 2.5 s (fourth one) and 0.6 s (fifth one). This procedure is illustrated by Fig. 25. For details of the decomposition method see Ref. [22].

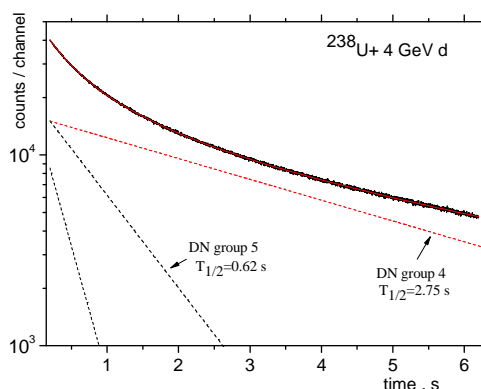


Figure 25: An expansion in the precursor groups of the DN spectrum measured at deuteron energy of 4 GeV.

In Fig. 26 the systematic of weight ratios [23-27] of the abovementioned groups in dependence on neutron energy for $^{238}\text{U}(n,f)$ - reaction is presented together with the results of analysis of present data (red circles with crosses inside). The blue circles indicate results obtained in June 2009 [22] with smaller (~300 kg natural uranium) target assembly which had a lead blanket of 10 cm thick.

As it follows from Fig. 26 for the studied uranium target assemblies the values of the mean neutron energy $\langle E_n \rangle$ inducing of ^{238}U nucleus fission are about (13 ± 4) and (35 ± 5) MeV for $E_d = 1$ and 6 GeV correspondingly. To test the sensitivity of this method to the change of the neutron energy spectrum in the active core the dedicated DN measurements on the target assembly ‘Energy + Transmutation’ (E+T) [28] had been carried out in November 2009 at deuteron energy of 4 GeV.

The (E+T) set-up consists of a central lead (\varnothing 8cm) target surrounded by 200 kg blanket

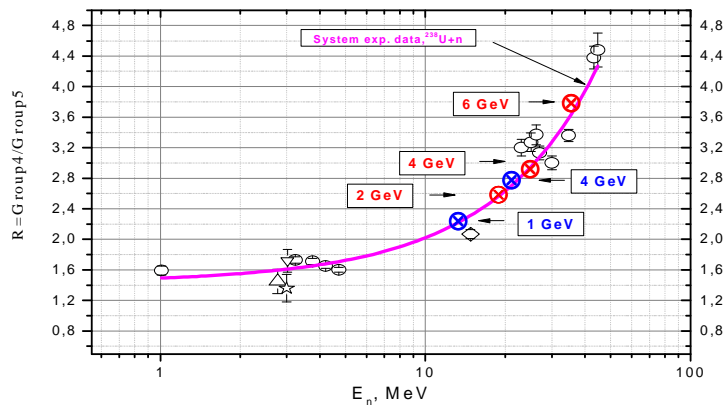


Figure 26: The neutron energy dependence of the ratios of DN groups for $^{238}\text{U}(n,f)$ -reaction [23-27] in comparison with the same ratios extracted from analysis of DN time spectra measured in 2009 and March 2011 NUCLOTRON runs.

from metallic natural uranium. Beside that the lead-uranium assembly was placed into thick (~300 mm) and dense ($\rho=0.7 \text{ g/cm}^3$) polyethelene box serving as a reflector and a moderator. In Fig.27 it is shown as the green curve the time dependence of neutron yield from the (E+T) target assembly measured by detector ISOMER-M in the same as in June 2009 geometry together with the respective spectra obtained for uranium and lead target assemblies [22] (red and blue curves respectively).

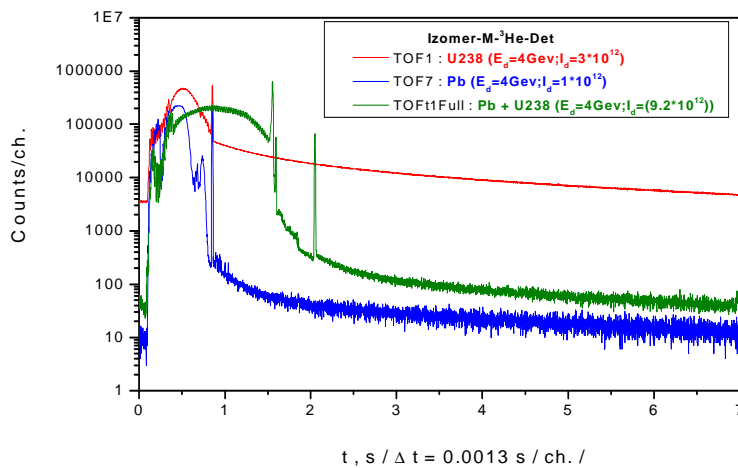


Figure 27: The time dependence of neutron yields from different target assemblies for $E_d = 4 \text{ GeV}$.

As it follows from Fig. 27 at the same beam energy the DN yield and respectively the number of fissions in the (E+T) target assembly is approximately by 2 orders of magnitude smaller than those obtained in June 2009 for 300 kg natural uranium target. This could be related with the usage of the intermediate lead target in the set-up (E+T) and also with the small thickness of the uranium blanket. Beside that a presence of the thick layer of polyethelene

surrounding the (E+T) target assembly has to make a resulting neutron spectrum softer in comparison with the same for the uranium target assembly that has no any moderator.

The analysis of DN time spectra measured for (E+T) target setup led to the result for $\langle E_n \rangle \sim 3$ MeV at $E_d = 4$ GeV. This is much lower than obtained above for TA QUINTA and reflects a real softening of the (E+T) neutron energy spectrum.

The DN time spectra obtained in all these measurements are formed in fission of target or blanket ^{238}U nuclei induced by the neutron flux $\varphi(E_n)$ inside of uranium volume. Roughly speaking the DN spectrum is determined by product of the fission cross section $\sigma_{nf}(E_n)$, the DN multiplicity $\nu_d(E_n)$ and the flux $\varphi(E_n)$. For $^{238}\text{U}(n,f)$ -reaction the product of $\sigma_{nf}(E_n) \nu_d(E_n)$ varies within several percents over a wide range of E_n , at least, up to $E_n \approx 15$ MeV. Therefore, the value of $\langle E_n \rangle$ obtained above can be considered as the realistic mean energy of neutrons initiating fission for studied target assemblies.

An integration of the DN time spectra reduced to one incident deuteron over whole measurement time range (1 - 7.6) s makes it possible to compare the relative total DN yields Y_{DN}^{tot} for different deuteron energies. These yields should be proportional to the total fission numbers discussed above. The obtained results arbitrary normalized at $E_d = 1$ GeV to the respective value of N_f^{tot} from Table 6 are given in Table 7.

Table 7. The relative DN total yields in comparison with the total numbers of fissions N_f^{tot} (in units of per one deuteron and 1 GeV).

Run	$E_d = 1$ GeV	$E_d = 2$ GeV	$E_d = 4$ GeV	$E_d = 6$ GeV	$E_d = 8$ GeV
	Total numbers of fissions N_f^{tot} (activation method)				
03.11		$(8.8 \pm 0.4) \pm 1.0$	$(8.8 \pm 0.4) \pm 1.0$	$(8.3 \pm 0.4) \pm 0.9$	
12,11	$(10.6 \pm 0.5) \pm 1.1$		$(8.5 \pm 0.4) \pm 1.0$		
03.12	$(10.5 \pm 0.5) \pm 1.1$		$(9.7 \pm 0.4) \pm 1.0$		$*(9.7 \pm 0.5) \pm 1.1$
	Relative delayed neutron yields Y_{DN}^{tot}				
03.12	$(10.5 \pm 0.6) \pm 1.1$ normalized		$(10.3 \pm 0.6) \pm 1.1$		$*(13.2 \pm 0.8) \pm 1.3$

*The values were obtained with the original Khar'kov group beam intensity (see Table 4). If one uses the weighted value of this intensity so respective numbers reduce by 30%

It is seen a satisfactory agreement in incident energy dependence between the Y_{DN}^{tot} values and the N_f^{tot} numbers. Note that a collimated solid angle of the detector ISOMER-M is directed at the middle of the second section while the activation and SST detectors were located in the gaps between the sections. But the influence of this difference can be seen as a minor.

To obtain the above results special measures have been taken to improve the reliability and accuracy of beam intensity monitoring. For series of measurements lasting approximately 2 hours in addition to on-line monitors the aluminum foils were used. A coincidence between two method was achieved. Here is appropriate to note that an essential increase of relative total DN yield between 1 and 4 GeV of deuteron energy observed in [22] could be caused by deficiency in monitoring of deuteron fluxes as it became clear now.

The measurement of prompt neutrons emitted during the accelerator burst with aid of the detector DEMON has not been successful in December 2011 and March 2012 due to very large background of high energy neutrons. For nearest NUCLOTRON run in December 2012 an optimal detector shielding was modeling and constructed so first confident information on high energy part ($E_n > 3$ MeV) of leakage neutron spectrum should be obtained.

3.5. Measurements of (n, γ), (n,2n) and (n,f)-reactions of ^{232}Th and $^{\text{nat}}\text{U}$ samples.

The additional natural uranium and thorium samples were installed within the QUINTA TA in order to investigate an influence of its hard neutron spectrum on reactions occurring inside. The cylindrical shaped samples of several tenths gram each were situated in the positions shown in Fig. 28.

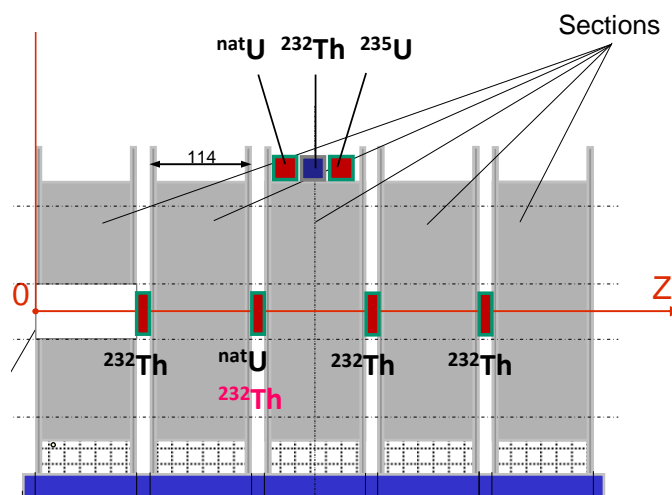


Figure 28: Location of uranium and thorium samples within QUINTA TA in measurements March 2012.

The samples were measured at deuteron energy of 2, 4 and 6 GeV without a lead blanket and at $E_d = 1, 4$ and 8 GeV with a blanket. By analyzing the gamma-ray spectra of irradiated $^{\text{nat}}\text{U}$ and $^{\text{nat}}\text{Th}$ samples, more than one hundred different residual nuclei have been reliably identified. A presence of many products of (n, γ), (n,2n) and (n,f) reactions was confirmed

during the analysis. More details of these experiments and data analysis are given in Ref. [29]. Below some preliminary results of measurements with these samples are presented.

In Fig. 29 the ratios of yields of ^{237}U and ^{239}Pu nuclei produced in reactions (n,2n) and

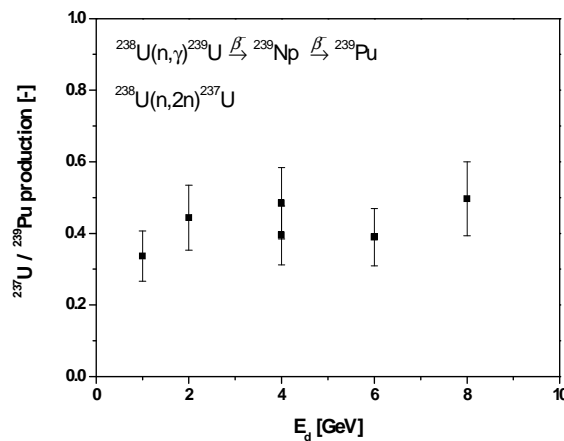
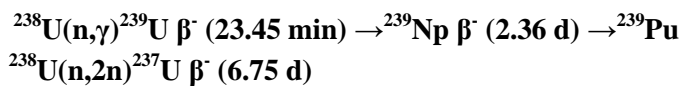


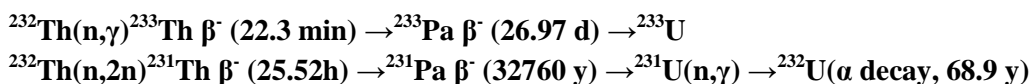
Figure 29: The ratios of the ^{237}U and ^{239}Pu nuclei production in neutron induced reactions on uranium sample located inside TA QUINTA.

(n,γ) on the ^{238}U nuclei accordingly are presented. The chains of respective reactions are as follows



Naturally, the values of these ratios are independent of the beam monitoring and provide qualitative information on dependence of neutron energy spectrum inside TA. If neutron radiative capture has no any threshold then the (n,2n) – reaction has a thresholds 6.18 MeV. Therefore, the practical constancy (within experimental errors) measured ratios $^{237}\text{U} / ^{239}\text{Pu}$ in the studied incident energy range indicates a slight change in the relation of hard and soft parts of the neutron spectrum on the axis of the target assembly.

In Table 8 the results of similar measurements for thorium samples are summarized. The chain of the respective reaction has the form



As the Table 8 shows the results for thorium are in general similar with the same presented above for uranium. Indeed the ratios of $^{232}\text{Th}(n,2n)^{231}\text{Th} / ^{232}\text{Th}(n,\gamma)^{233}\text{Th}$ and $^{232}\text{Th}(n,\gamma)^{233}\text{Th} / ^{232}\text{Th}(n,f)$ reaction rates are constant within their uncertainties in the studied deuteron energy range. However the experimental errors are too large to make quantitative conclusions. But the

reduced (to 1 GeV of E_d) fission rates show no change in dependence of incident energy in accordance with results discussed above in Subsection 3.3.

Table 8. Results of measurements of reaction rates for thorium samples (in units [E-27] the number of produced residual nuclei, per second, per one sample atom and per one incident deuteron). The errors shown in brackets do not include the uncertainties of beam doses.

Reactions -or ratios	$E_d = 2$ GeV	$E_d = 4$ GeV	$E_d = 6$ GeV
$^{232}\text{Th}(n,\gamma)^{233}\text{Th}$	76.9(39)	142(4)	176(3)
$^{232}\text{Th}(n,2n)^{231}\text{Th}$		51.4(15)	71.2(23)
$^{232}\text{Th}(n,f)$	54.4(40)	118(10)	159(7)
$^{232}\text{Th}(n,2n)^{231}\text{Th}/^{232}\text{Th}(n,\gamma)^{233}\text{Th}$		0.36(10)	0.40(11)
$^{232}\text{Th}(n,\gamma)^{233}\text{Th}/^{232}\text{Th}(n,f)$	1.42(1.2)	1.20(13)	1.11(6)
$^{232}\text{Th}(n,f)/E_d$	27.2(20)	29.5(2.5)	28.5(1.2)

The spectral indexes obtained in these measurements (second bottom row in the Table 8) are essentially larger than the respective values discussed for ^{238}U in Section 3.2. The last ones were about (0.3 – 0.4) in the same measurement position. The difference may be due to a higher threshold of the $^{232}\text{Th}(n,f)$ -reaction. But this item needs more careful verification.

4. Discussion of the results

One of the major problems of our experiments is the lack of quantitative information on neutron field inside the target assembly. Only way to obtain information on neutron spectra and its variation inside of TA volume is to use the technique of threshold activation detectors. Such measurements have been realized during last NUCLOTRON runs but processing of this data is rather cumbersome and does not completed up to now. The preliminary results of the spatial distribution of normalized threshold reaction rates R measured in the gap between second and third sections during March 2012 run are shown in Table 9.

The R values are given in special units for easy data analysis. The measured reaction rates (i.e. a number of produced residual nuclei per second and per one target nucleus N_t) were multiplied by the square of the distance r from the beam axis and the corresponding cross-sections were reduced to one barn. Beside that all R values were normalized to one incident deuteron and divided by its energy in GeV. Such normalization of the reaction rates allows one to compare the actual neutron flux in the distance scale and the energy scale. The most of the threshold reactions used in the measurements have approximately a bell-shape dependence of their cross-sections on neutron energy. So it is possible to consider the value of the normalized reaction rate as a measure of the average magnitude of the neutron flux (per one deuteron and 1

GeV) in the given point within the target volume at an energy threshold of the respective reaction.

Table 9. Spatial distributions of the normalized threshold reactions R in depending from deuteron energy (in units $[E-29] \cdot r^2 \cdot N_t^{-1} \cdot \sigma^{-1} \cdot s^{-1} \cdot d^{-1} \cdot \text{GeV}^{-1}$).

Reaction	σ , b	r , cm	Ed, GeV		
			1	4	8
$^{58}\text{Ni}(n,p)^{58}\text{Co}$	0.16	$E_{\text{th}} = 0.90 \text{ MeV}$			
		4	770±80	620±65	726±80
		12	1450±160	1163±120	1485±150
		32	877±90	1128±120	2696±300
$^{59}\text{Co}(n,p)^{59}\text{Fe}$	0.016	$E_{\text{th}} = 3.45 \text{ MeV}$			
		4	273±30	258±30	296±30
		12	412±45	432±43	710±80
		32	403±43	416±42	432±45
$^{24}\text{Mg}(n,p)^{24}\text{Na}$	0.07	$E_{\text{th}} = 6.15 \text{ MeV}$			
		4	191±22	168±18	159±16
		12	276±29	274±30	283±29
		32	366±39	281±32	314±32
$^{59}\text{Co}(n,2n)^{58}\text{Co}$	0.38	$E_{\text{th}} = 11.05 \text{ MeV}$			
		4	90±10	61±7	74±8
		12	125±14	117±13	104±11
		32	127±14	131±14	137±14
$^{209}\text{Bi}(n,4n)^{206}\text{Bi}$	0.434	$E_{\text{th}} = 24.95 \text{ MeV}$			
		4	62±7	46±5	56±6
		12	79±9	79±8	135±14
		32	71±9	88±9	124±13
$^{209}\text{Bi}(n,5n)^{205}\text{Bi}$	0.356	$E_{\text{th}} = 33.35 \text{ MeV}$			
		4	49±6	39±4	48±5
		12	73±9	61±7	117±13
		32	121±15	73±9	91±10
$^{209}\text{Bi}(n,7n)^{203}\text{Bi}$	0.205	$E_{\text{th}} = 54.75 \text{ MeV}$			
		4	55±7	34±5	33±4
		12	48±6	55±7	69±7
		32	63±8	63±7	64±7

Analysis of the data from the Table 9 shows that in inner region of TA ($r \leq 12$ cm) a “shape” of neutron spectra does not change much up to the threshold energy of 11 MeV. The similar behavior of the “effective” neutron flux on a surface of the lead blanket ($r = 32$ cm) is observed excluding may be most soft part of neutron spectrum ($E_{th} = 0.16$ MeV). For the threshold energy $E_{th} = 24.95$ MeV only at $r = 4$ cm there is no dependence of the “shape” of neutron spectra from deuteron energy. For larger distances from beam axis at $r = 12$ and 32 cm the neutron spectrum becomes harder with growing of deuteron energy. Much more uncertain is the neutron flux behavior at high threshold energies. This region requires the use of other methods of investigation. There are some hopes that necessary information will be obtained in forthcoming December 2012 run of NUCLOTRON with aid of Si detectors located within TA QUINTA.

Significant information about changing the neutron spectra inside the target can be obtained from the dependence of the spatial distributions of the spectral indices on the incident deuteron energy. The typical results of respective measurements are shown in Fig. 30.

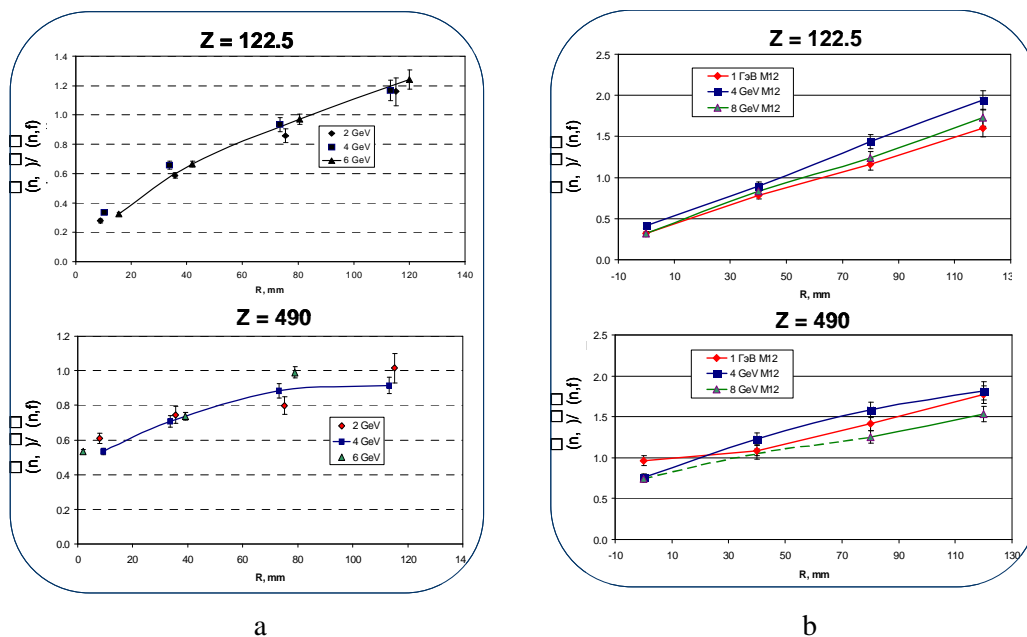


Figure 30: Radial distributions of spectral indices for different Z positions measured for $E_d = 2, 4$ and 6 GeV in March 2011 (a) and for $E_d = 1, 4$ and 8 GeV in March 2012 (b). The curves are drawn for easier comparison only.

It is appropriate to remind here that values and uncertainties of spectral indices do not depend on an accuracy of measurement of the beam flux. As shown in Fig. 30 the spectral indices increase essentially with grows of distance from the beam axis. This behavior reflect a softening of neutron energy spectrum with increasing radial distance. The magnitude of the increasing becomes smaller for larger Z values. All studied spectral indices show practically no

dependence within the experimental errors on deuteron energy. So, respectively, the shape of neutron energy spectra has minor variations inside TA QUINTA with increasing incident energy. But it is seen dramatic changes in the values of studied indices and its radial and axial variations caused by adding the lead blanket to TA QUINTA. This means that the lead blanket returns back mainly leaked neutrons from the soft part of their energy spectrum. Therefore, we can assume that in quasi-infinite uranium AC the equilibrium neutron energy spectrum should be softer than in the multiplying target of smaller diameter such as TA QUINTA.

The second unsolved question of the conducted experiments is a leakage of neutrons from TA QUINTA and their energy spectrum. These neutrons are lost for fission of target nuclei and for the ^{239}Pu isotope production. So for a correct estimation of the beam power gain in the studied TA QUINTA one needs in reliable information on value of neutron leakage. Some indirect information on this subject can be obtained by comparing of the radial dependence of integral fission yield $Y_f^{int}(r)$ calculated on the basis of data [8] and on the results of our measurements. In Fig. 31 the respective $Y_f^{int}(r)$ values are given in arbitrary units.

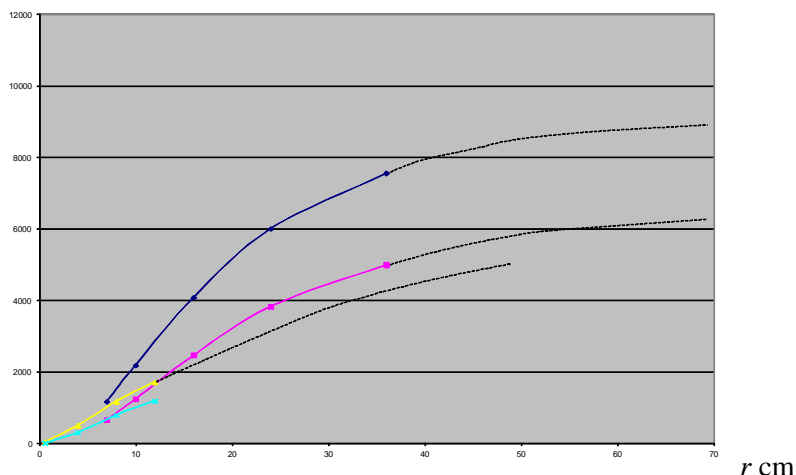


Figure 31: Comparison of radial dependence of integral fission yield $Y_f^{int}(r)$ in quasi-infinite AC [8] (blue and purple curves) with the same in QUINTA TA (yellow and light blue ones).

A difference between the blue (yellow) and purple (light blue) curves is due to the fact that they are calculated for $Z = 24.5$ cm and 65.5 cm, respectively. An interpolation for $r > 30$ cm is made internally because of the lack of necessary data in Ref. [8].

An analysis of radial dependences of integral fission yields from [8] shows that the neutron leakage at $r = 15$ cm is $\sim (55-60)\%$. Accounting for difference in uranium densities of AC of Ref. [8] and of TA QUINTA one can estimate the value of leakage of neutrons from TA QUINTA as $\sim (80-90)\%$. But this conclusion has to be tested by direct measurements planned for December 2012 run.

Some information on possible size of quasi-infinite TA in our experimental conditions can be obtained from Fig. 31 too. Because the radial dependence of integral fission yield tends to saturate it is possible to conclude, that the target radius of 60 cm corresponds to a quasi-infinite metal uranium AC. This is just the radius of BURAN TA available for future experiments. However, it should be noted that above estimates of the size of a quasi-infinite target for energy of incident particles greater than 1 GeV may be larger because of the possible increase with growing of incident energy the average energy of spallation neutrons.

Taking into consideration the beam power gain (BPG) estimated on the basis of results of Ref. [8] (see discussion in Section 2 above) and accounting for a linear dependence on incident energy of the total fission yield from TA QUINTA in the studied range of deuteron energy (1 – 8) GeV we can obtain as low limit for BPG of quasi-infinite AC the value ~ 8.

Note that for the limited size of TA QUINTA having a neutron leakage about 80% the BPG is ~ 2. This result is in good agreement with a direct measurement of BPG done in Ref. [30]. In this experiment the target setup from metallic depleted uranium with a diameter of 20 cm and a length of 57 cm irradiated by protons of energy (0.8 – 1.2) GeV. There was measured the heat from practically complete absorption of the proton beam inside the target. So at an incident energy of 1 GeV the value of BPG has turned to 2, 17 ± 0.16 in good agreement with the respective estimates obtained for TA QUINTA.

It is appropriate to compare our data with calculations of Ref. [31]. Authors of this paper attempted to assess the possibilities of RNT and concluded that given approach can not achieve its goals. For calculation in Ref. [31] there was used the model target setup shown in Fig. 32.

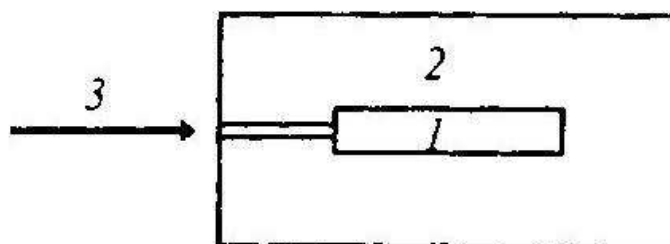


Figure 32: Model ADS setup: 1 – the target (depleted uranium, ϕ 20cm, L= 100cm), 2 - blanket (depleted uranium, ϕ 100cm, L= 200cm), 3 - proton beam. Target mass ~ 30 tons.

The results obtained in Ref. [31] are presented in Table 10. Here E_p is the proton energy, Q – a total energy release in the target, M_n – a neutron multiplicity and $\langle E_n \rangle$ is a mean energy of neutron spectrum within the target. The total numbers of fissions N_f are divided into two parts induced by neutrons with energies greater than 14 MeV, and less.

If one compares the beam power gain at a proton energy E_p of 1 GeV shown in Table 10 with the same values from Ref. [8] obtained at $E_p = 0.66$ GeV for the depleted uranium target

Table 10. Main characteristics of the model ADS calculated in Ref. [31].

E_p , GeV	Q , GeV	Beam Power Gain	N_{Pu}	N_f $E_n > 14 \text{ MeV}$	N_f $E_n < 14 \text{ MeV}$	M_n	$\langle E_n \rangle$ MeV
Uranium (depleted) target + Uranium(depleted) blanket							
1	3.27	3.27	68.6	2.93	12.7	44.6	3.05
10	29.8	2.98	609	26.5	113	403	3.05
40	102	2.54	1930	83.9	358	1260	3.01
Lead target + Lead blanket							
1	0.64	0.64		0.029	171	34.4	3.02
10	6.27	0.63		0.12	1550	292	3.06
40	27.3	0.68		0.44.1	5000	934	3.03

assembly of equivalent mass ~ 7 t so an essential difference is revealed. In Ref. [8] BPG ≈ 6 is about two times more than the respective number from the above Table.

The calculated in [31] the mean energy of neutron spectra $\langle E_n \rangle$ at least for the lead target seems to be too small in comparison with the respective value obtained in experiment of Ref. [32] for the extended lead target. Results of this experiment are given in Table 11.

Table 11. The characteristics of neutron field produced in the lead target ($\phi 20 \times 60 \text{ cm}$) by protons of energy in the range (1-3.65) GeV (data from Ref. [32]).

$E_p, \text{ GeV}$	$\langle E_n \rangle, \text{ MeV}$	$E_{kin}, \text{ MeV}$	$E_{kin}/E_p, \%$	$W, \text{ MeV}$	$W/E_p, \%$
0.99	8.82	213	21.3	382	38.2
2.0	11.6	513	25.6	822	41.1
3.65	13.7	116	30.3	1670	45.6

Here W/E_p is a share of beam energy E_p expended in the formation of neutrons, E_{kin} – a kinetic energy is carried away by the neutrons and $\langle E_n \rangle$ is a mean energy of neutron spectrum. It is seen that the measured value of $\langle E_n \rangle$ increases with growing of proton energy in contrary with results of Ref. [31] shown in Table 10. May be this difference is related to the limited size of the target used in measurements [32]. But in any case only dedicated experiments with really quasi-infinite uranium target such as BURAN setup can provide comprehensive information about feasibility of the RNT approach in future ADS applications.

Very essential for search of the optimal incident energy in studied ADS is the result given in Table 11, namely, the growth of the beam energy share W/E_p consumed in the formation of

neutrons. The high value of W/E_p and its significant growth of proton energy provide an incentive to expand the range of incident energies in future experiments.

An important aspect of RNT approach feasibility is the increase in concentration of the ^{239}Pu isotope in the active core up to its equilibrium level in the long-term operation of the respective ADS. In dependence of this level the beam power gain can increase up to an order of magnitude preserving low enough value of k_{eff} (a more detailed discussion, see Ref. [1]).

In this connection it is useful to discuss the results of the paper [33] in which the ADS with quasi-infinite AC from depleted uranium and without moderator has been theoretically investigated for incident proton energy of 1 GeV. To find the neutron field $\Phi(r, z)$ authors used a single-group diffusion approximation under the condition of a stationary incident beam and isotropic external source of neutrons. Of the many channels of hadronic processes of primary and secondary intranuclear cascades it was taken into account only the fission of uranium AC by protons. Essential limitation of this study was using as model neutron spectrum the respective spectrum of fast reactor with an average neutron energy of about 0.2 MeV, which is significantly different from the real neutron spectrum of any ADS. Despite this lack the results of calculations of the equilibrium plutonium concentration and a dynamics of its change are interesting. The obtained value of this concentration itself is not so significant because of the above-mentioned disadvantages of the calculation scheme. But the estimates of the time to achieve this equilibrium concentration for a given proton current are useful. These results show good perspectives for realization of RNT.

5. Conclusion

In course of implementation of JINR project “Energy and Transmutation RAW” during last two years in the frame of large international collaboration a basic physics of interaction of high energy deuterons with massive uranium target assembly QUINTA was studied. Main obtained results as well the used experimental technique were presented above. These results provide solid grounds for planning of future experiments with quasi- infinite target setup of depleted uranium BURAN available for the “Energy and Transmutation RAW” collaboration at JINR. But data obtained in measurements with QUINTA TA can be interesting as a self-sufficient basis for bench-mark calculations aimed at verification of respective codes dedicated for description of interaction of high energy particles with massive multiplying targets.

The authors express their sincere gratitude to the NUCLOTRON team for fruitful cooperation in the measurements, and thank the directorate of JINR Veksler-Baldin Laboratory of High Energy Physics for the effective support in the preparation and implementation of our experiments.

References

- [1] A.A. Baldin, E.M. Belov, M.V. Galanin et al., *Nuclear relativistic technologies (RNT) for energy production and utilization of spent nuclear fuel. Results of first experiments on physics justification of RNT, Particles and Nuclei, Letters*, **6** (2011) 1007 (in Russian); *JINR Preprint E1-2011-24*, Dubna 2011 (in English)
- [2] H. A. Abderrahim, P. Baeten, D. De Bruyn et al, *MYRRHA, Multipurpose hybrid Research Reactor for High-end Applications, Nuclear Physics News*, **20** (2010) 24
- [3] V.V. Chilap et al, *The problems of development of worldwide nuclear power on the relativistic nuclear technologies (RNT) (in Russian)*, <http://www.cftp-aem.ru/Data/RADS02.pdf>
- [4] A.S. Bogomolov, *BWLAP - Backward Wave Linear Accelerator of Protons, in proceedings of Int. Linac Conf.*, **2**, (1994) 789, Tsukuba, Japan.
- [5] J.W. Weale, H. Goodfellow, M.H. McTaggart and M.L. Mullender, *Measurements of the reaction rate distribution produced by a source of 14 MeV neutrons at the centre of a uranium metal pile, Journal of Nuclear Energy, Parts A&B*, **14** (1961) 91
- [6] D.L. Wang, *China Nuclear Science Report (in Chinese) CNIC-00506 SINPC-0001* (1991)
- [7] S. Andriamonje, A. Angelopoulos, A. Apostolakis et al., *Experimental determination of the energy generated in nuclear cascades by a high energy beam. Physics Letters B*, **348** (1995) 697
- [8] R.Vassil'kov, V.Gol'dansky, B.A. Pimenov and Yu.N. Pokotilovsky, *Multiplication of neutrons in uranium irradiated by protons with energy 300-660 MeV, Atomic energy*, **44**, (1978) 329 (in Russian)
- [9] R. Jian, *Brief Report on the Testing Calculation of the Fission Rate for the ^{238}U , Communication of Nuclear Data Progress, CNDC 0027*, **23** (2000) 150
- [10] A.A. Smirnov and A.D. Kovalenko, *Nuclotron – superconducting nuclei accelerator at LHE, JINR (design, operation and development), Particles and Nuclei, Letters*, **1**, 6(123) (2004) 10
- [11] N.A. Gundorin, K.V. Zhdanova, V.E. Zhuchko et al., *Measurement of delayed neutron yield from fission of ^{237}Np by thermal neutrons, Phys. At. Nucl.*, **70**, 6, (2007) 1011
- [12] J. Frána, *Program DEIMOS32 for Gamma-Ray Spectra Evaluation, J. Rad. Nucl. Chem.*, **257**, 3 (2003) 583
- [13] M. Majerle, *Monte Carlo Methods in Spallation Experiments, PhD thesis, FNSPE CTU Prague*, (2009) (<http://ojs.ujf.cas.cz/~wagner/transmutace/diplomky/mitjathesis.pdf>)
- [14] H. Kumawat, *Development of Cascade Program and its Applications to Modeling Transport of Particles in Many Component Systems, PhD Thesis*, (2004) JINR Dubna.
- [15] O. Svoboda, *Experimental Study of Neutron Production and Transport for ADTT, PhD Thesis, FNSPE CTU, Prague*, 2011, (http://ojs.ujf.cas.cz/~wagner/transmutace/diplomky/PHD_Svoboda.pdf)
- [16] V. Hnatowicz, *Handbook of Nuclear Data for Neutron Activation Analysis*, **1**, Czechoslovak Atomic Energy Commission – Nuclear Information Centre, 57-805/86, (1986) Prague

- [17] J. Banaigs et al., *Determination De L'Intensite D'Un Faisceau De Deutons Extrait D'Un Synchrotron Et Mesure Des Sections Efficaces Des Reactions C-12(D,P2N)C-11 Et Al27(D,3P2N)Na-24 a 2.33 GeV*, *Nuclear Instruments and Methods in Physics Research*, **95** (1971) 307
- [18] P. Kozma P. and V.V. Yanovski, *Application of BaF₂ scintillator to off-line gamma ray spectroscopy*, *Czech Journal of Physics*, **40** (1990) 393
- [19] V.A. Voronko, V.V. Sotnikov, V.V. Sidorenko et al., *Generation of neutrons in uranium-lead target assembly at irradiation by deuterons of 1.6 GeV energy*, *Problems of atomic science and technology. Series: Nuclear Physics Investigations* **47** (2008) 174 (in Russian)
- [20] S.R. Hashemi-Nezhad, I. Zhuk, A.S. Potapenko et al., *Calibration of track detectors for fission rate determination: An experimental and theoretical study*, *Nucl. Instrum. Methods in Physics Res., Sect.A.* **568** (2006) 816.
- [21] M.Yu. Artyshenko, V.A. Voronko, K.V. Husak et al., *Measurements of deuteron beam parameters on QUINTA target setup with aid of SSTD*, *this Proceedings*.
- [22] W. Furman, A. Baldin, N. Gundorin et al., *Time-dependent spectra of neutrons emitted by interaction of 1 and 4 GeV deuterons with massive natural uranium and lead targets*, *Journal of Korean Physical Society* **59** (2011) 2006
- [23] R. W. Waldo et al., *Phys. Rev.*, **C23**, (1981) 1113
- [24] L.Tomlinson, *Rep. AERE-R 6993* (1972).
- [25] C. B. Besant et al. *J. Br. Nucl. En. Soc.*, **16**, (1977) 161.
- [26] H. Rose and R. D. Smith. *J. Nucl. Energy*, **4**, (1957) 133.
- [27] 14. S. G. Isaev. *Ph.D. thesis*, IPPE, Obninsk (2001) (in Russian).
- [28] M.I. Krivopustov, D. Chultem, J. Adam et al., *On a First Experiment on the Calometry of an Uranium Blanket Using the Model the U/Pb Electro-Nuclear Assembly "Energy Plus Transmutation"*, *Preprint JINR P1-2000-168*, Dubna (2000) (in Russian); *Kerntechnik*, **68**, (2003) 48
- [29] L. Zavorka, J. Adam, M. Kadykov et al., *A summary of the experimental results on reactions in the uranium samples irradiated with a deuteron beam of energies up to 8 GeV at the QUINTA target*, *this Proceedings*
- [30] V.I. Belyakov-Bodin, V.D. Dubinsky, V.D. Kazaritskii et al., *Calorimetric measurements and Monte-Carlo analysis of interaction of intermediate energy proton beam with uranium target*, *Atomic Energy*, **70** (1991) 339 (in Russian)
- [31] V.F. Batyaev, M.A. Butko, K.V. Pavlov et al., *Analysis of basic nuclear-physics peculiarities of proton beams interaction with heavy metallic targets*, *Atomic Energy*, **104** (2008) 242 (in Russian)
- [32] V.I. Yurevuch, R.M. Yukovlev, V.A. Nikolaev et al., *Study of Neutron Emission in Interactions of Relativistic Protons and Deuterons with Lead Targets*, *Particles and Nuclei, Letters*, **3** (2006) 49

- [33] E.V. Gusev, P.A. Demchenko and L.I. Nikolai'chuk, *Proton beam driven subcritical reactor with a combined target, VANT, series "Plasma electronics and new acceleration methods"*, **4** (2004) 27 (in Russian)